Molecular Biology and Evolution, XXXX, pp. 1–27

doi: DOI HERE
Advance Access Publication Date: Day Month Year
Paper

PAPER

The genetic architecture of venom resistance: a novel approach to target identification and coevolutionary discovery

Micaiah J. Ward,[1] Schyler A. Ellsworth,[1] Elizabeth G. King,[2] Enoch Ng'oma,[2] Gunnar S. Nystrom,[1] Kylie C. Lawrence,[1] Lauren Maquet-Diafouka,[1] Alex Oliver,[1] Mark J. Margres,[3] Christopher L. Parkinson,[4] Kimberly A. Hughes[1] and Darin R. Rokyta[1,*]

[1]Department of Biological Science, Florida State University, Tallahassee FL, USA, [2]Division of Biological Sciences, University of Missouri, Columbia, MO, USA, [3]Department of Integrative Biology, University of South Florida, Tampa, FL, USA and [4]Department of Biological Sciences, Clemson University, Clemson SC, USA
[*]Corresponding author. drokyta@bio.fsu.edu
FOR PUBLISHER ONLY Received on Date Month Year; revised on Date Month Year; accepted on Date Month Year

Abstract

All species evolve under selective pressures that emerge from their interactions, often antagonistic, with other species. Phenotypes mediating species interactions manifest as the combined products of the genomes of interacting species; understanding the evolutionary processes acting in one lineage therefore cannot be attained without bridging the genomes of interacting species. Venoms have arisen independently more than 100 times in animals and serve diverse roles in species interactions, including predation and defense. Each venom is evolutionarily entwined with reciprocal phenotypes, such as venom resistance, in often diverse recipient species. Despite extensive work on venoms, the full genetic basis for resistance to whole venoms is largely unknown. Using the venom of the Florida blue centipede (*Scolopendra viridis*) comprised of 35 toxins and *Drosophila melanogaster* as model prey, we investigated the genetics of venom resistance for a naive prey through experimental evolution and genetic-mapping approaches. We identified 12 consensus genes across techniques associated with venom resistance, yet individual experiments suggested a genome-wide basis for resistance involving hundreds to thousands of genes, despite the relative simplicity of the venom of *S. viridis*. We found no evidence for fitness trade-offs associated with the evolution of resistance and revealed a stark contrast in the nature of venom resistance between prey sexes. The disparity in resistance genetics between prey sexes as well as the relative genetic complexity of venom versus resistance may ultimately give venomous predators a coevolutionary advantage over their prey.

Key words: Venom, Resistance, Experimental Evolution, Coevolution, *Drosophila*

Introduction

Coevolution, reciprocal evolutionary change between species, plays a central role in generating and maintaining adaptive variation (Lenski 1984; Thompson 2005), but most studies focus on morphology (Parchman and Benkman 2002; Toju 2008) or relatively simple systems. Although interactions that drive coevolution occur at phenotypic interfaces (Brodie III and Brodie Jr 1999; Smith and Benkman 2007; Dawkins 2016), a mechanistic understanding of coevolutionary dynamics requires understanding the genetics dictating the outcomes of these interactions (Thompson 2013), which has remained challenging

for all but the simplest systems (Medina *et al.* 2022). Coevolutionary dynamics at the molecular level in natural populations have perhaps been best characterized in newts (genus *Taricha*) and garter snakes (genus *Thamnophis;* Geffeney *et al.* 2002; Feldman *et al.* 2009). Newt toxicity is matched by toxin resistance in predatory garter snakes, which results from repeated amino-acid substitutions in certain ion channels (McGlothlin *et al.* 2016). Yet this arms race involves a single toxin and a few ion channels; most traits mediating species interactions emerge from many loci (Wellenreuther and Hansson 2016), and coevolutionary dynamics are highly dependent on the genetics of interacting traits (Ebert 2018; Gallinson *et al.* 2024; Clement *et al.* 2025).

The relative genetic complexities of interacting traits could, in part, determine coevolutionary outcomes. Orr (2000) showed that the rate of adaptation declines with increasing complexity of the system under selection. Complex organisms pay a cost of complexity resulting from a reduced probability that mutations will be beneficial (Fisher 1930), reduced probabilities of fixation of beneficial mutations, and smaller fitness gains per beneficial substitution. All else being equal, the member of a pair of antagonistically interacting species with the genetically simplest coevolutionary trait should be able to out-evolve the other. Empirical evidence for this cost of complexity is lacking (McGee *et al.* 2016; Sackman and Rokyta 2019; Houle and Rossoni 2022), and phenomena such as modularity and particular patterns of pleiotropy and mutational effect sizes could ameliorate or even eliminate this cost of complexity (Wang *et al.* 2010; Wagner *et al.* 2008; Houle and Rossoni 2022). Nonetheless, the relative complexities of traits mediating interactions represent critical information for understanding and modeling coevolutionary dynamics.

Venomous animals represent 15% of all animal diversity (Holford *et al.* 2018), and each species produces a unique mix of tens to thousands of bioactive molecules that destructively interfere with the fundamental molecular functions of their intended venom recipients. Venoms function solely following injection into another organism, resulting in direct species interactions. The extensive variation in venoms (Margres *et al.* 2015; Ward *et al.* 2018a; Margres *et al.* 2019) is often attributed to coevolution with prey, but the full genetic basis of venom resistance is unknown (Holding *et al.* 2016). Previous work in venoms has focused largely on single toxin-gene/resistance-gene interactions (Jansa and Voss 2011; Rowe *et al.* 2013; Gibbs *et al.* 2020), similar to what has been done in other coevolving systems (Geffeney *et al.* 2002; Feldman *et al.* 2009). Unlike the garter snake and newt system, where a single toxin is involved, venoms are cocktails of numerous toxins; the multifarious and synergistic activities of its components likely make the genetic basis for resistance far more complex. A systems-level analysis of venom and resistance is therefore needed to determine how the relative genetic complexities of interacting traits affect coevolutionary dynamics. Recent work using whole-genome CRISPR knockout screens against box jellyfish (Lau *et al.* 2019) and cobra (Du *et al.* 2024) venoms in human cell lines shows promise for identifying genes involved in manifesting the cytotoxic activity of venoms, but this approach does not capture the tissue- and organism-level context of venom effects.

Selection on natural prey will, over time, purge variation in genes contributing to resistance, rendering them invisible to mapping approaches (Märkle *et al.* 2021). Naive prey provide a complete view of resistance genes unobscured by past selection, whereas natural prey can reveal the subset of genes driving ongoing coevolutionary dynamics. These characterizations are complementary; both are relevant to understanding coevolution. We characterized a novel, experimental predator-prey relationship using the giant Florida blue centipede (*Scolopendra viridis*) and a naive prey species, fruit flies (*Drosophila melanogaster*). We took a multifaceted approach, including whole-genome sequencing and venom proteomics of *S. viridis* (Figure 1) and both evolve and resequencing (E&R, Figure 2) and extreme quantitative trait loci (XQTL) analyses in *D. melanogaster*, to comprehensively identify toxins and their targets in a whole-venom, whole-animal model system. We first established substantial heritable variation in venom resistance in the *Drosophila* Synthetic Population Resource (DSPR; King *et al.* 2012b) fly lines and reasoned that experimental evolution of a mixed population constructed of these lines could reveal the genetic architecture of resistance to a complex venom. In addition, we utilized a mixed *Drosophila* Genetic Resource Panel (DGRP; Fochler *et al.* 2017) population in an XQTL framework to independently investigate resistance genetics and provide added confidence in venom target identification. Our results revealed that the genetic architecture of venom resistance is rich with complex phenomena including a lack of apparent fitness trade-offs, potential sex-specific resistance mechanisms, and variable adaptive genetic pathways among replicate populations under the same selective pressures.

Results

The venom of *Scolopendra viridis*

To understand the relationship between the genetics of venom and venom resistance, a complete characterization of venom genes is a critical starting point. Ward and Rokyta (2018) identified 39 proteomically confimed toxins for *S. viridis* using

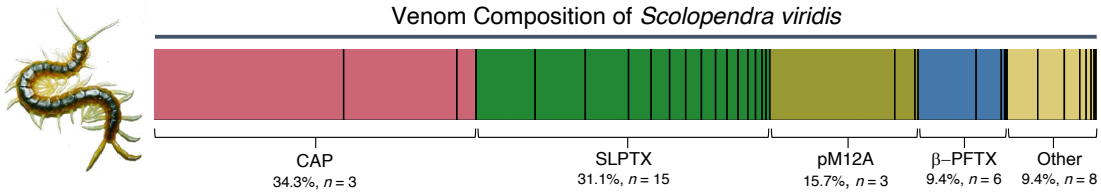

Fig. 1. The venom of *S. viridis* is predominantly comprised of four toxin families: CAP (cysteine-rich secretory proteins [CRISPs], antigen 5 [Ag5], and pathogenesis-related 1 [Pr-1]), SLPTX (scoloptoxins), pM12A (metalloproteases), and β-PFTX (β-pore-forming toxins). Other toxins include low abundance venom proteins (Table S1).

de novo transcriptome assembly of two RNA-seq data sets. A subsequent re-analysis of these data by Ellsworth *et al.* (2024) found 38 proteomically confirmed toxins for each of the two individuals. Transcriptomic and proteomic approaches can fail to resolve the true complexity of venom by collapsing closely related paralogs, leading to an underestimate of venom complexity. Alternatively, such approaches can overestimate complexity by the *in silico* creation of chimeric sequences or by failing to differentiate allelic variation from copy-number variation. Recent work has leveraged high-accuracy long-read sequencing (*i.e.,* PacBio HiFi) to completely resolve tandem arrays of venom loci in snakes (Margres *et al.* 2021; Myers *et al.* 2022; Hogan *et al.* 2024; Nachtigall *et al.* 2025). To establish a link between venom and resistance genes, we comprehensively characterized the venom of *S. viridis* by producing a high-contiguity genome assembly (contig $N50$ = 48.5 Mbp) based on ∼33× PacBio HiFi reads and using previously published RNA-seq and venom mass-spectrometry data (Ward and Rokyta 2018; Ellsworth *et al.* 2024). We identified 35 venom components and estimated their proteomic abundances (Figure 1; Table S1). Our results qualitatively agree with previous characterizations, with the major venom components being cysteine-rich secretory proteins (CRISPs), antigen 5 (Ag5), and pathogenesis-related (PR-1) superfamily proteins (CAPs), as well as scoloptoxins (SLPTXs), metalloproteases (pM12As), and β-pore-forming toxins (β-PFTXs).

Two approaches to determining resistance genetics

Our two primary approaches to characterizing the genetics of venom resistance, evolve and resequencing (E&R) and extreme quantitative trait loci (XQTL) analysis, are complementary but differ in some critical details which affect interpretation of their results. Both approaches are based on selection for survival of venom injection in genetically diverse populations. We used independently derived lineages of *D. melanogaster* for each approach, ensuring that the specific alleles (*i.e.*, SNPs) available differed between the two sets of experiments and thereby improving the robustness of our results. For the XQTL approach, we applied one round of selection for survival and directly genotyped survivors (*i.e.*, selection without evolution). For the E&R approach, we allowed multiple generations of evolution and therefore introduced the possibility that pleiotropy and epistasis could impact the results. The E&R approach is more likely to detect mutations that are at low frequencies in the initial population, but also less likely to detect mutations with resistance effects that have trade-offs with other life history traits, because the surviving flies must still reproduce and produce viable offspring for the next generation. In addition, the XQTL experiments rely solely on existing genetic variation, but the E&R approach allows for the possibility of the introduction of new mutations.

Establishing genetic variation of venom resistance in naive prey

Genetic variation for resistance to *S. viridis* venom was measured by assessing the phenotypic response to venom injection (*i.e.,* alive vs. dead) among 192 recombinant inbred lines (RILs) from the *Drosophila* Synthetic Population Resource (DSPR; King *et al.* 2012b). Male *D. melanogaster* were more sensitive to venom injection compared to females (see Methods; Table S2), resulting in using sex-specific venom doses of 1.87 ng/mg (males) and 2.20 ng/mg (females). We found significant ($p < 0.0001$) among-RIL variance in *D. melanogaster* and broad-sense heritabilities of 0.281 in females and 0.428 in males (Figure S1; Tables S2 and S3), effectively establishing genetic variation of venom resistance in *D. melanogaster*.

Although the purpose of evaluating venom resistance among RILs was to establish genetic variation for this trait, we also attempted QTL mapping (King *et al.* 2012b; Marriage *et al.* 2014) with these data. Despite the administration of a lower venom dose, male *D. melanogaster* exhibited higher mortality rates compared to females and did not offer an adequate distribution for reliable QTL mapping (see Methods; Figures S2 and S3; Table S2). In female *D. melanogaster*, we identified a single significant

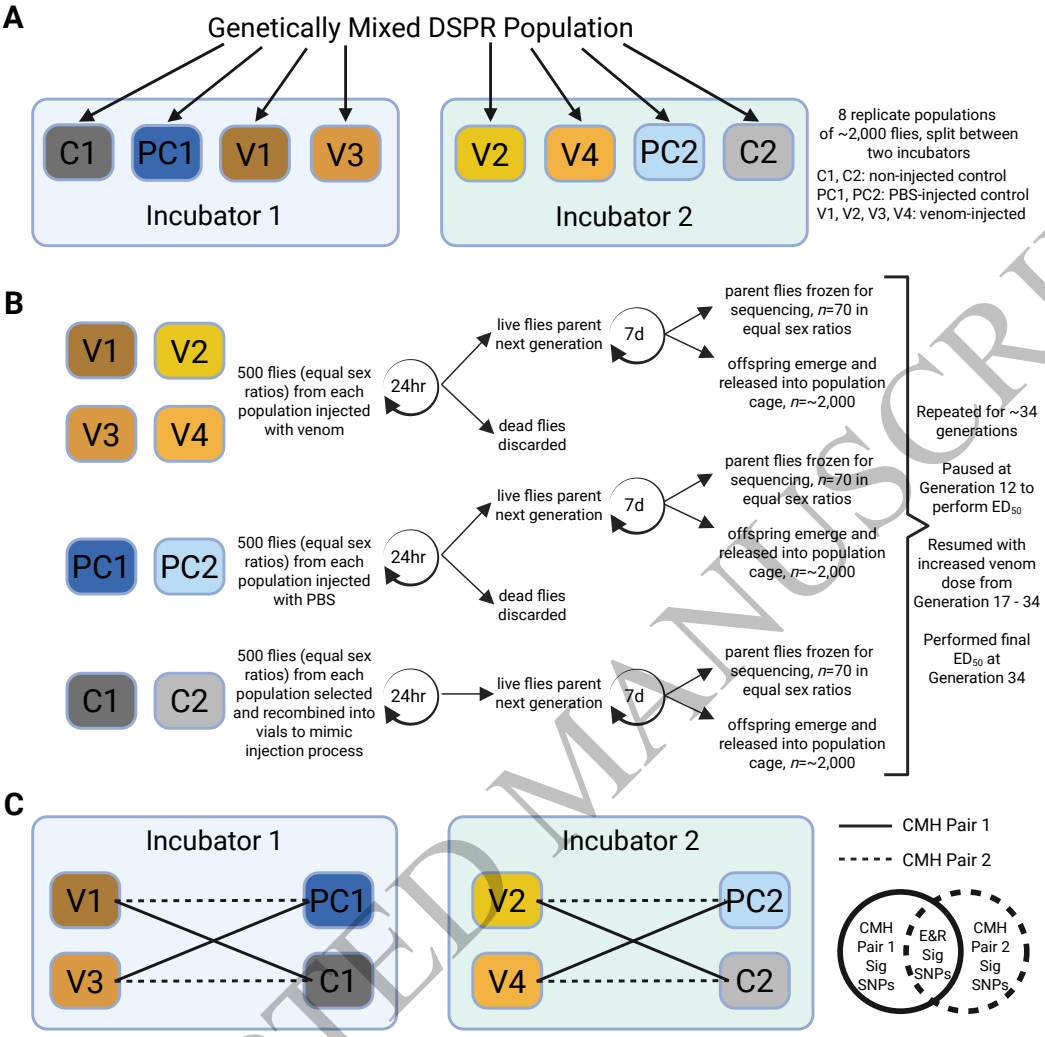

Fig. 2. Evolve and resequencing experimental design. (A) 835 DSPR RILs were used to establish a genetically mixed population and subsequently seed eight replicate populations ($N = 2,000$), with four replicates in each of two incubators. Each incubator contained one non-injected control replicate, one PBS-injected control replicate, and two venom-injected replicates. (B) At each selection event, 500 flies (250 males, 250 females) were selected for injection with venom (V1–V4), injection with PBS (PC1, PC2), or non-injected (C1, C2). After a recovery period of 24 hours, dead flies were discarded and live flies were recombined to parent the next generation. After seven days, parent flies were removed and preserved for sequencing. The successive generation for each replicate was released in a population cage. After three days, bottles of media seeded with eggs were removed from the population cages and emerged offspring were used for the next round of selection. (C) To identify significant SNPs, each venom-injected replicate was paired with each control replicate within each incubator to perform Cochran-Mantel-Haenszel (CMH) statistical tests, resulting in two test pairs per incubator (CMH Pair 1 test: V1-C1, V3-PC1, V2-C2, V4-PC4; CMH Pair 2 test: V1-PC1, V3-C1, V2-PC2, V4-C2). For each generation, a SNP was only considered significant if the same SNP was identified as significant in both test pairs (see Methods). Created with BioRender.com.

QTL associated with venom resistance, encompassing a region that included 1,137 protein-coding genes and spanned the centromere on chromosome 3 (Figures 3 and S3). Due to low recombination in centromeric regions (Denell and Keppy 1979), many of these genes were likely in linkage disequilibrium (LD) with causal sites and not causal themselves. Therefore, we did not consider these genes as venom targets on the basis of these data alone.

Experimental evolution of venom resistance

After confirming substantial heritable variation in venom resistance in DSPR fly lines, we established a genetically mixed population of *D. melanogaster*

from 835 DSPR RILs (Ng'oma *et al.* 2019) to select for venom resistance (Figure 2A). A single venom dose of 0.47 ng/mg was used for both male and female *D. melanogaster* of the DSPR mixed population to achieve a starting 50% lethality rate in venom-injected replicates. Although the death rate among venom-injected replicates seemed to decrease rapidly and stabilize after six rounds of selection (Figure 4A), we did not find a significant difference in median effective dose (ED_{50}) values between the venom-injected replicates and the control replicates by this time (approximately 12 generations; Figure 4B). However, the initial dose of 0.47 ng/mg was no longer effective at achieving a 50% lethality rate across venom-injected replicates (Figure 4A). We therefore used an increased venom dose of 0.55 ng/mg (Figure 4C) and continued selection for another 20 generations (approximately 10 rounds of selection). At this time point (generation 34), the ED_{50} values of the venom-injected replicates had significantly increased compared to the control replicates (p = 0.0316, average venom-injected replicate ED_{50} = 0.972 ng/mg, average control replicate ED_{50} = 0.570 ng/mg; Figure 4; Table S6), confirming increased venom resistance across four replicate populations of *D. melanogaster*.

The evolve and resequencing (E&R) results revealed a genome-wide response to selection for venom resistance, implicating 6,126 candidate genes with potential association to venom resistance (Figure 3; Tables S5 and S15) and suggesting a genetically complex response to selection (Barghi *et al.* 2020). We incorporated time-series (Barghi *et al.* 2020) and haplotype structure (King *et al.* 2012b) analyses by sequencing a subset of individuals from each venom-injected and control population at generations 12 and 34, corresponding with where we saw the greatest changes in phenotypic response (Figure 4; Tables S6 and S7). Because we found a significant incubator effect when establishing genetic variation among DSPR RILs (Table S3), we identified significant SNPs for each generation 12 and 34 by performing two Cochran-Mantel-Hanzel (CMH) tests per generation, such that each venom-injected replicate was paired and cross-paired to each control replicate (PBS-injected and non-injected) within the same incubator (Figure 2C). The resulting overlap of significant SNPs from these two tests were deemed the significant SNPs for each generation. Therefore, a SNP was only identified as significant in our analysis if it was significantly divergent across venom-control pairs and across incubators. Significance thresholds were based on p-values for the 99.99^{th} percentile in three replicate data simulations of our experimental design (see Methods), and these simulations were also used to calculate false discovery rates (FDRs) for our experimental results (Table S4). By generation 12 of the E&R, 38,585 SNPs were identified as significantly diverged between venom-injected and control populations (FDR < 0.0220), corresponding to 5,672 genes (Figure 6; Table S5). By generation 34, the number of significant SNPs reached 66,506 (FDR < 0.0142) corresponding to 6,126 genes. Among these, 5,864 significant SNPs (FDR < 0.0004) corresponding to 1,570 genes were common to both generations (Figure 6; Table S5). Our haplotype structure analysis found non-overlapping genome regions between generations 12 and 34 (Figure 3; Tables S5 and S15) that exhibited significant differences in haplotype frequencies in the venom-injected versus control replicates. Although we found variation in genetic response among replicate populations, with a large number of significant SNPs contributing to this variation (Figures S6 and S7; Tables S16 and S17), our goal was to better understand the overarching genetic impact of evolved venom resistance. We therefore focused on consistent differences in venom versus control replicates in our analysis and did not identify target genes within each venom-injected replicate individually.

Life-history trait associations with venom resistance

The sex-specific response to venom injection observed in the DSPR RILs prompted us to assess any obvious costs associated with evolved venom resistance in the DSPR mixed population throughout the E&R. To accomplish this, we measured three key *D. melanogaster* life-history traits: emergence time, weight, and number of offspring produced, and tested whether these traits were impacted by selection for venom resistance versus the PBS-injected controls (Figure 5). As in the RILs, males in the DSPR mixed population experienced higher mortality in response to venom injection relative to females (Table S8). However, unlike the RILs, the same venom dose was used in both male and female *D. melanogaster* in the E&R. We found no evidence of trade-offs associated with venom resistance evolution in measured life-history traits of emergence time or number of offspring. We did find a significant association of fly weight and selection over time (p=0.0170), but there was no significant difference between venom-injected and PBS-injected groups (p=0.555). Interestingly, when looking at the weights of males and females separately (data not shown, but see Table S8), only the females showed a significant relationship of weight and selection over time (p=0.0101), and this association was due to a decrease in weight over time. As we found no significant difference in weight between venom-injected and PBS-injected females (p=0.372), this suggests that weight has little or no impact on response to venom injection and that other experimental variables contributed to female weight decrease over time. As males did not experience significant weight changes over time (p=0.123) nor

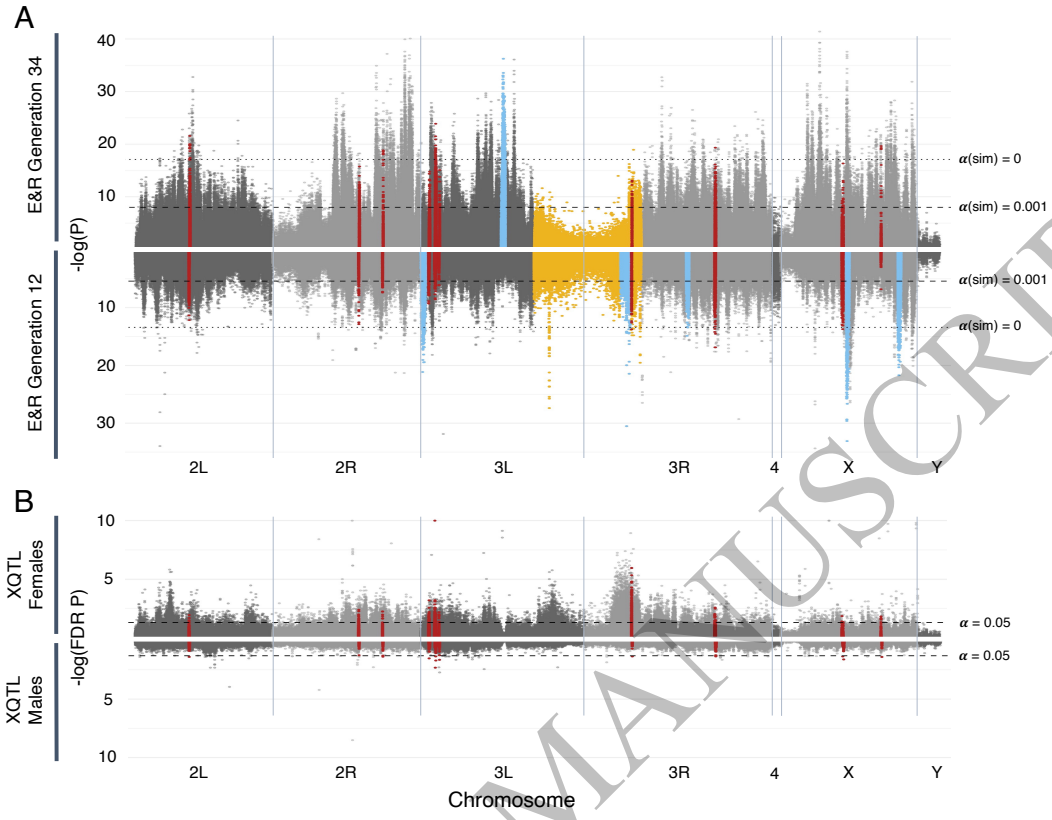

Fig. 3. Even a simple venom engenders genome-wide adaptive (E&R) and genic (XQTL) architecture of venom resistance. In Manhattan plots, red regions represent regions containing the 12 primary candidate genes in common to both E&R and XQTL data. Light blue regions represent significant haplotype regions found in the E&R, and the gold region represents the QTL. (A) E&R plots at generations 12 (bottom) and 34 (top) from the DSPR mixed population, $\alpha(\text{sim}) = 0$ represents the most significant p-value among simulated replicates, $\alpha(\text{sim}) = 0.001$ represents the highest p-value corresponding to the 99.9$^{\text{th}}$ percentile among simulated replicates and was used as our significance threshold (see Methods; Figure S4; Table S4). (B) XQTL plots for males (bottom) and females (top) from the DGRP Flyland II population, an $\alpha = 0.05$ represents the p-value corresponding to the 95$^{\text{th}}$ percentile of FDR corrected p-values.

was there a significant difference between venom-injected and PBS-injected groups in males (p=0.931), this result further suggests that the sex-specific venom sensitivity observed in male *D. melanogaster* is not due to their smaller size.

Extreme Quantitative Trait Loci (XQTL) mapping in an independent genetic background

We independently confirmed the genetically complex nature of venom resistance by observing changes under a single round of selection in the *Drosophila* Genetic Resource Panel (DGRP) based Flyland II mixed population (Fochler *et al.* 2017) using XQTL mapping, which can identify putative SNPs that could be eroded by the more long-term forces of genetic drift and purifying selection (Fochler *et al.* 2017; Zhou *et al.* 2017; Anholt and Mackay 2018; Kurlovs *et al.* 2019; Barghi *et al.* 2020). Because XQTL mapping is a one-time selection event aimed at capturing the most resistant individuals, we first determined the 80% effective lethal dose (ED_{80}) separately for male and female *D. melanogaster* from the DGRP Flyland II population. The resulting ED_{80} doses were 3.1 ng/mg for males and 7.5 ng/mg for females. Each XQTL selection event was performed in duplicate for each fly sex. Significant SNPs were those that were identified as significantly divergent between the base population and venom-injected survivors using the CMH test with an FDR corrected p-value threshold of 0.05. Our XQTL results further emphasized a potential sex-bias in response to venom, both phenotypically and genetically (Figure 3), with only 70 significant SNPs corresponding to 61 genes identified in males, compared to 19,862 significant SNPs in 4,431 genes in the females (Figure 6).

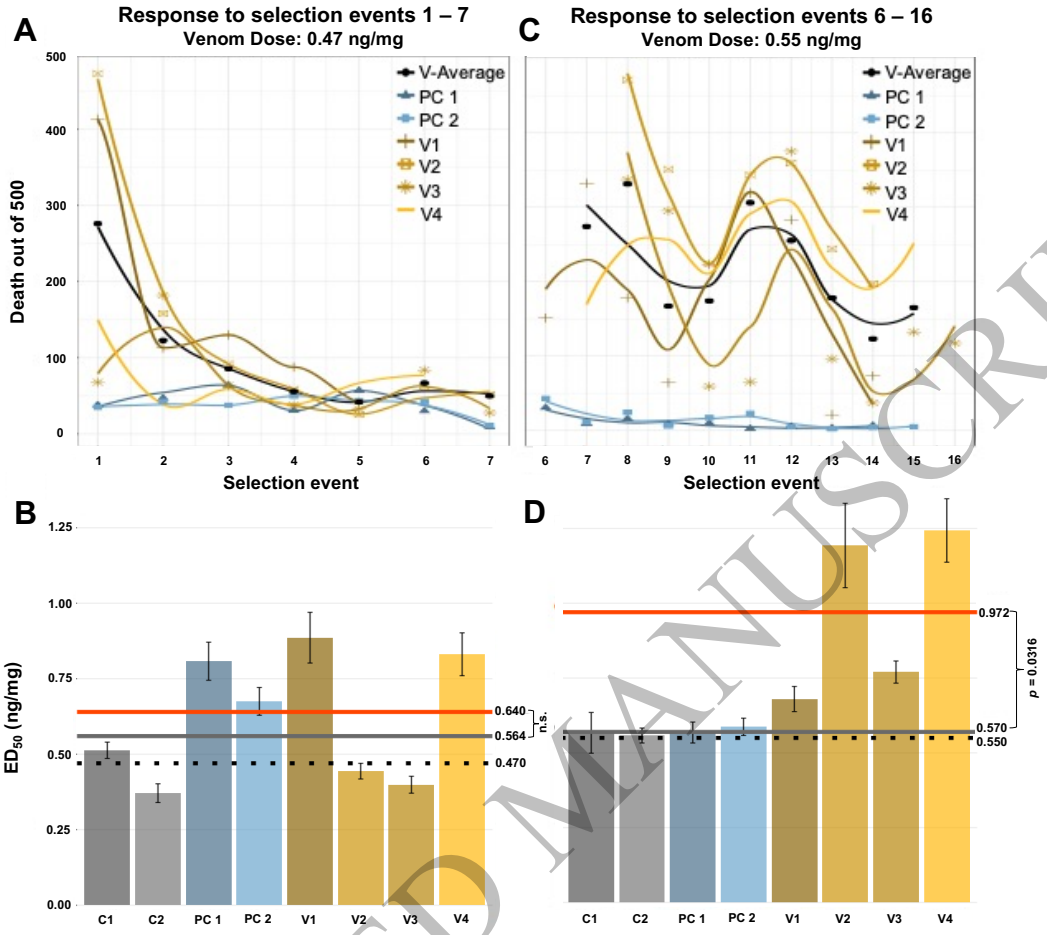

Fig. 4. Phenotypic response to selection for venom resistance over time. Selection events took place every 2–3 generations and involved injecting 500 individual *D. melanogaster* (250 males and 250 females) with *S. viridis* venom. Values of death for each selection event are provided in Table S7, and ED_{50} values in Table S6. (A) Although the initial response to selection for venom resistance was variable (V1–V4), the average death among all venom-injected replicates (V-Average) decreased from 55.2% to 10.0% over selection events 1–7 using a dose of 0.47 ng/mg. (B) ED_{50} values with standard deviation (sd) error bars for each non-injected control (C1–C2), PBS-injected control (PC1–PC2), and venom-injected (V1–V4) replicate after approximately seven selection events (12 generations) using a venom dose of 0.47 ng/mg (dotted line) indicated no difference in the means of venom-injected (red line, 0.640 ng/mg) and control (grey line, 0.564 ng/mg) replicates ($p = 0.698$). (C) Response to selection for venom resistance using increased dose of 0.55 ng/mg shows variation in response among replicates and selection events, although the average death among all venom-injected replicates (V-Average) decreased from 54.8% to 33.0% by the final selection event. (D) Final ED_{50} values with sd error bars for each non-injected control (C1–C2), PBS-injected control (PC1–PC2), and venom-injected (V1–V4) replicate after approximately 15 selection events (34 generations) using a venom dose of 0.55 ng/mg (dotted line) indicates a significant difference in the means of venom-injected (red line, 0.972 ng/mg) and control (grey line, 0.570 ng/mg) replicates ($p = 0.0316$).

The average sequencing coverage for female replicates (148.8×) was higher than for males (87.0×; Table S11). To determine whether this difference could account for the observed difference in resistance genetics between the sexes, we re-ran our analyses after subsampling reads for each replicate down to the number for the lowest-coverage replicate across sexes. Normalizing read counts across all replicates decreased the number of significant genes in males from 61 to 45 and decreased the number of significant genes for females from 4,431 to 908. Although coverage differences accounted for part of the magnitude of the difference in numbers of significant genes, females still showed more than an order of magnitude more genes after accounting for this discrepancy. This pattern, in addition to the differences in sensitivity to venom between male and

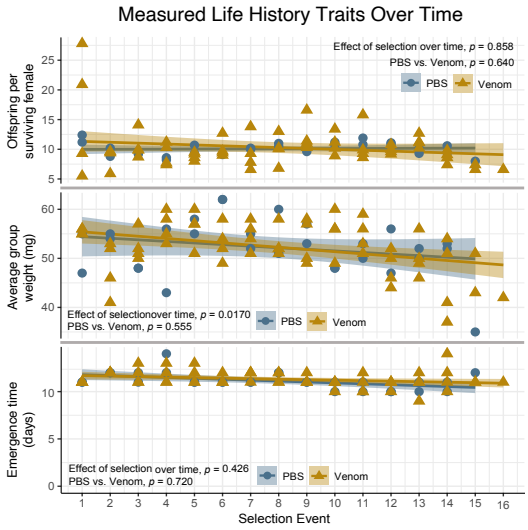

Fig. 5. Measured life history traits indicated no obvious costs or trade-offs associated with evolved resistance. We found no significant relationship in number of offspring per surviving female (throughout selection $p = 0.858$; between V and PC replicates $p = 0.640$), or in emergence time (throughout selection $p = 0.426$); between V and PC replicates $p = 0.720$). We found a significant difference in the average weight over the course of selection ($p = 0.0170$), but not between venom-injected and PBS-injected groups ($p = 0.555$), suggesting the decrease in average fly size was independent of venom resistance selection.

female flies, suggests a real biological basis for the sex specificity in venom response.

Venom target identification

We took a conservative consensus-based approach to venom target identification by combining results across approaches and identified a set of 12 primary candidate genes with a high probability of being biologically meaningful for venom resistance. These 12 genes were consistent among the most independent forms of analyses (E&R and XQTL), with common SNPs identified in the two E&R time points and corresponding genes also identified in both sexes in the XQTL (Figures 3 and 6; Table 1). Because we identified substantially more genes in the XQTL female data compared to the males, we considered the 739 genes identified in both E&R generations and in the female XQTL our secondary candidate genes (Figure 6; Table S5). A network analysis of primary candidate genes closely connected six (*tai, baz, spri, Ptp61F, Svil, dsx*) of the 12 primary candidate genes as well as a number of secondary candidate genes (Figure S8), providing evidence that selection may be acting on the same gene network, where individuals may have one variant or another of a given gene within the network. The 12 primary candidate genes were dispersed throughout the genome, representing all major chromosomes (Figure 3, red regions). Two genes on chromosome 3L (*Spn* and *Svil*) and two genes on the X chromosome (*spri* and *X11Lbeta*) represent the closest genetic locations among the primary candidate genes, but neither of these gene pairs are functionally paired in the same interaction network (Figure S8).

Discussion

Although identifying genes underlying the production of venoms has become routine with modern approaches (Margres *et al.* 2021; Myers *et al.* 2022; Hogan *et al.* 2024), finding the genes on which they select in venom recipients' genomes has proven to be far more challenging. We introduced three new approaches to aid in deciphering the venom-mediated genome-genome interactions that arise from the mechanisms of action of whole venoms. One of these, classical QTL mapping using RILs, was severely underpowered in our implementation and resulted in the identification of a single significant genomic region for female *D. melanogaster* (Figure 3). Although the inclusion of additional RILs would certainly have increased our power, ultimately this approach will not be easily scalable for broad applicability. Our E&R approach revealed the staggering complexity of venom resistance and that resistance can evolve quickly with no evidence of fitness trade-offs in common life-history traits. Our XQTL approach provided an independent confirmation of the complexity of venom resistance, while also allowing us to separately assay male and female flies to demonstrate a stark difference in both venom susceptibility and resistance genetics between sexes. Altogether, we have revealed several novel patterns in the genetics of venom resistance. First, natural populations can harbor substantial genetic variation for resistance. Second, venom resistance is far more genetically complex, potentially involving more than 1,000 genes, than venom itself (35 toxins). Third, despite this complexity, venom resistance can evolve rapidly with little evidence for fitness trade-offs. Finally, prey sexes can experience venom-based selection differently, which could potentially hinder their evolutionary response.

The genetic architecture of venom resistance

The venom of *S. viridis*, comprised of just 35 proteins (Figure 1), is a relatively simple venom. If each venom component had a single target in prey, we would expect a correspondingly simple genetic basis for venom resistance. In establishing genetic variation for venom resistance in *D. melanogaster*, we simultaneously identified a single QTL in females alone, which is consistent with a simple genetic architecture of venom resistance, although additional RILs would be required to increase the power to perform a full genome-wide association study

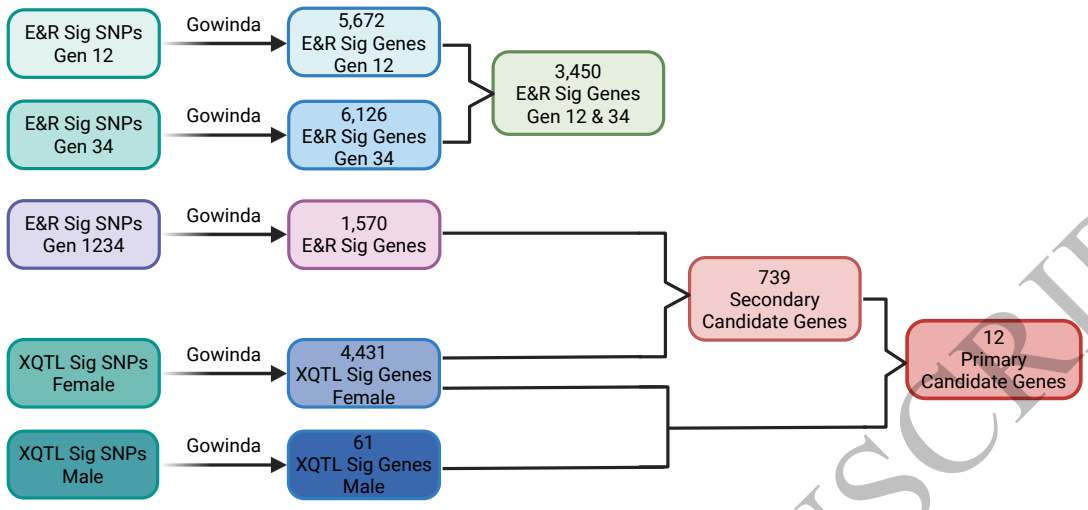

Fig. 6. Identification of primary candidate genes. Genes containing significant SNPs at each generation 12 and 34 of the E&R, significant SNPs in common to generation 12 and 34 of the E&R, and significant SNPs in each sex of the XQTL were identified using Gowinda. 1,570 genes shared common significant SNPs in both generation 12 and 34 of the E&R. Of these, 739 genes were common with the XQTL female significant genes and considered secondary candidate genes. A total of 12 primary candidate genes shared significant SNPs in generations 12 and 34 of the E&R and were also identified as significant genes in both males and females of the XQTL. Created with BioRender.com.

(GWAS). Contrary to our QTL results, the E&R and XQTL approaches revealed a genome-wide response to selection for venom resistance involving 61 (male XQTL) to 1,570 (genes with common significant SNPs in both E&R time points) and possibly more genes (Table S5), pointing to a more complex genetic architecture. Time-series analyses have been shown to increase the power to detect true positive alleles under selection and in distinguishing between selective sweep (few, strong loci) and polygenic (many, small-effect loci) architecture adaptation models in E&R studies (Barghi *et al.* 2020). Therefore, we included two time points in our E&R corresponding with the greatest phenotypic change in response to venom injection, which allowed us to identify lasting targets of selection for venom resistance, and, in combination with our haplotype analysis, support a more dynamic and complex genetic response over time. Together, these results may suggest a more parallel selection signature among replicates at earlier time points where haplotype structure is more likely intact, and greater variation among replicates at later time points where they may be sorting into new and unique genetic optima. Indeed, variation in genetic response among replicate populations was present in our data (Figures S6 and S7; Tables S16 and S17) and has been observed elsewhere (Barghi *et al.* 2019). Although genetic drift, LD, and genetic draft (Nuzhdin and Turner 2013) cannot be ruled out as contributors to this variation, these effects were minimized by our experimental design and significance thresholds (see Methods; Figure S4; Table S4). The lack of retained haplotype structure in our E&R also suggests high levels of recombination and decreased LD over time, further minimizing these impacts on our results. Considering that venoms are a cocktail of proteins, peptides, and small molecules, each venom component has the potential to impose selection on its own or synergistically with variable selection strengths, which may influence the genetic response (Kofler and Schlötterer 2014) and contribute to the observed genome-wide complexity. Together, our results point to genetic redundancy being a likely contributor to the large number of significant SNPs/genes and among-replicate variation, where replicates under the same selective pressure evolve alternate mechanisms of resistance while presenting the same phenotype. Our genetically independent extreme QTL (XQTL) mapping in the Flyland II *D. melanogaster* population (Fochler *et al.* 2017) also revealed a complex, genome-wide response to selection for venom resistance. XQTL mapping provides a powerful test to detect potential candidate genes involved in a single selection event, identifying SNPs that may be eroded by the more long-term forces of genetic drift and purifying selection (Fochler *et al.* 2017; Zhou *et al.* 2017; Anholt and Mackay 2018; Kurlovs *et al.* 2019; Barghi *et al.* 2020). Therefore, alleles identified with the XQTL approach may contribute to variation in resistance without necessarily being adaptive due to pleiotropic effects, whereas those identified under an E&R approach should increase fitness overall. By using a combined approach, we identified consistently selected SNPs

throughout the E&R in genes that were also identified as significant the XQTL, giving greater chance of these genes being selected from standing genetic variation across populations and contributing to increased venom resistance.

The approaches we used to characterize resistance genetics, E&R and XQTL, are powerful, but they have their limits. Finite sample sizes, stochastic effects, and the amount of genetic variation, as well as its distribution in the populations and genomes, can result in both false positives (*e.g.*, through linkage or drift) and negatives (*e.g.*, due to low power to detect rare alleles). Nonetheless, by focusing on the consensus signal among replicates and approaches and being conservative in our significance thresholds, we endeavored to minimize false positives. We therefore view our characterizations as incomplete and conservative, but far more comprehensive than previous work. If, as Orr (2000) predicted, complex traits suffer a cost of complexity in terms of their evolutionary rates, then our results suggest one means by which venomous predators may gain an evolutionary advantage over their prey. The venom of *S. viridis* is comprised of 35 toxins (Figure 1), yet resistance genetics for this venom in *D. melanogaster* likely involves one or two orders of magnitude more genes (Table S5).

Sex-specificity and costs of venom resistance

In establishing genetic variation of venom resistance among DSPR RILs, we found that male *D. melanogaster* were more susceptible to venom injection relative to females. We found, however, too little variation in response among males to perform QTL analysis. Although initially thought to be due to the size difference between male and female *D. melanogaster*, the sex-specific difference in venom susceptibility remained true when the venom dose was adjusted for weight in the DSPR RIL and XQTL experiments, and, in the E&R, females remained more resistant even as their weight decreased over time. In addition to these phenotypic results, our XQTL results revealed extreme genetic differences in response to venom injection between males and females. Similar results were reported in an XQTL study aimed at identifying genes associated with resistance to heavy metal toxicity (Zhou *et al.* 2017), indicating resistance mechanisms in general may be sex-specific. Indeed, sex-biased susceptibility presents a confounding variable in the context of potential fitness consequences (Connallon *et al.* 2010) and implicated diseases (Morrow and Connallon 2013) and may also have relevance in coevolving populations (Holding *et al.* 2020).

In host-parasite coevolution, hosts are known to show sex-specific responses to parasites (Zuk and McKean 1996; Duneau *et al.* 2012). Host sexes can differ in, for example, immune responses (Gipson and Hall 2016), morphology, hormonal composition, physiology, life history, and behavior, each of which could impose differing selective pressures on parasites. Depending in part on sex ratios in hosts, parasites are predicted to either evolve host-sex-based dimorphism, specialize on one sex, or evolve host-sex-based phenotypic plasticity (Duneau and Ebert 2012). Host sexual dimorphism can impede adaptation of parasites, particularly in well mixed populations with equal sex ratios, but can also provide an evolutionary advantage to parasites when alleles yielding an advantage to one sex decrease fitness in the other (Duneau and Ebert 2012). In our analogous predator-prey scenario, we established that some aspect of *D. melanogaster* sexual dimorphism results in dramatically different venom susceptibility and allelic effects across prey sexes. For the XQTL experiments, male and female flies should have had the same alleles in the same frequencies (aside from those on the sex chromosomes), and yet we detected orders of magnitude more resistance-related genes in females than males with minimal overlap (Table S5). Of the 4,431 genes identified in females and 61 in males, only 36 were in common between the sexes. Given the consistency in nearly all aspects of the XQTL experiments in male and female *D. melanogaster* (Table S11), we have little reason to suspect that the sex differences detected are technical, rather than biological. Sequencing coverage differed between the sexes (Table S11), but, by re-analyzing the data after normalizing read counts across samples, we showed that the signal for sex-specificity remained after accounting for this difference. We cannot determine the extent to which the sex-specific genes merely have reduced benefits in the other sex, with the difference thereby resulting from differential power, as opposed to fitness costs. Regardless, these patterns and the differences in venom susceptibility suggest that were this form of predator-prey interaction to occur in nature, the evolutionary dynamics and outcomes would depend on prey sex ratios and encounter rates and could potentially benefit either species, depending on the specific populations and interactions. Our results therefore implicate another layer of complexity that must be considered to understand venom-mediated coevolution.

One phenomenon that may be contributing to the sex-specificity of venom resistance observed here is genome-wide sexual conflict, which can produce high quality offspring of the same sex and lower quality offspring in the opposite sex, resulting in the maintenance of genetic variation for fitness in the presence of strong selection (Foerster *et al.* 2007; Cox and Calsbeek 2009). Sexually antagonistic selection is common in wild populations and the favoring of opposing alleles between sexes can result in balancing selection which can maintain stable polymorphisms in

homogeneous environments (Cox and Calsbeek 2009; Fry 2010; Mank 2017). With respect to insecticide resistance in *Drosophila*, sexual conflict occurs in the locus for resistance which, in addition to resistance, provides a reproductive benefit in females, but is costly in males (Rostant *et al.* 2015; Hawkes *et al.* 2016). Using an experimental evolution approach, Hawkes *et al.* (2016) found that balancing selection was occurring at this locus, with resistant females showing a higher fitness and males showing little effect from the resistance locus. Similar work has been shown in red deer where sexually antagonistic selection differentially effects the fitness of sexes sired where successful males sired daughters that were less successful and had a lower breeding value, while sons had no decrease in correlation to their father (Foerster *et al.* 2007). We identified a different number of causal SNPs for males and females in the XQTL analysis that could reflect differences in genetic optima for venom resistance. If sexually antagonistic selection is acting on venom resistance in *D. melanogaster*, it could limit the adaptive potential for this trait by maintaining genetic variation which could reduce the effects of directional or sexual selection. Furthermore, and perhaps surprisingly, we found no evidence of trade-offs or costs of evolved venom resistance over time, though only a small number of traits were able to be adequately measured in this study.

Targets of venom resistance

Our primary candidate genes consist of nuclear, cytosolic, and membrane-bound targets, many with roles in common physiological responses to envenomation (*i.e.*, immune, sensory, and neurological responses), indicating that our results are biologically, not just statistically, meaningful. Based on their known or predicted functions (Table 1), *Mctp*, *Ptp61F*, and *SKIP* have the most obvious connections to *S. viridis* venom resistance. The *Mctp* gene encodes a Multiple C2 domain and transmembrane region protein that enables Ca^{2+} binding at neuronal synapses. As confirmed here and previously (Ward and Rokyta 2018; Ellsworth *et al.* 2024), *S. viridis* venom is predominantly composed of CAPs, which are known Ca^{2+} channel toxins. Resistant variants of *Mctp* could help stabilize synaptic function and reduce overall debilitating symptoms of envenomation. The *Ptp61F* gene encodes protein tyrosine phosphatase 61F, which functions as a negative regulator of the JAK-STAT pathway, an established key regulator of inflammatory and stress responses. As a negative regulator of this pathway, knockout of *Ptp61F* has been shown to increase JAK-STAT activity (Baeg *et al.* 2005); therefore, enhanced PTP61F activity could protect against toxin-induced hyperactivation of JAK-STAT. The *SKIP* gene is not well characterized, but as a K^+ interacting protein, may respond to the predominantly K^+-channel targeting SLPTXs present in *S. viridis* venom (Ward and Rokyta 2018; Ellsworth *et al.* 2024). We identified three genes, *baz*, *mspo*, and *Svil*, with potential roles in defensive barriers and/or wound healing. Epithelial barriers, in particular, are critical for immune defense in *D. melanogaster* (Davis and Engström 2012), and β-PFTXs are abundant in centipede venoms, including *S. viridis* (Ward and Rokyta 2018; Ellsworth *et al.* 2024). Although their exact function in venom remains to be elucidated, they are hypothesized to form pores in cellular membranes, potentially with cell or receptor-type specificity (Knapp *et al.* 2010; Dal Peraro and Van Der Goot 2016). Identification of genes that maintain cell structure integrity via cell polarization, cytoskeleton organization, and tissue remodeling supports the hypothesis that β-PFTXs target and disrupt membrane barriers, although further validation would be necessary to confirm. Although not as well characterized as *Mctp*, we identified additional genes with predicted roles in central nervous system (CNS) regulation. Both *Spn* and *X11Lbeta* have predicted activities in synaptic zones and are likely responding to neurotoxic venom components. Based on its human orthologs, *CG11537* may be involved in transport of folate or associated nutrients essential in CNS function, and venom toxins may target this gene to disrupt motor or cognitive function of prey. The remaining primary candidate genes identified in our analysis are not as easily functionally associated with evolved venom resistance. The *tai* gene encodes a steroid hormone receptor coactivator and has multiple roles in transcription and metabolic regulation as well as locomotion. The connection between *tai* and evolved venom resistance is unclear, though previous work has indicated *tai* expressing cells are able to both evade death signals through immune signalling repression and also kill neighboring cells (Byun *et al.* 2019), suggesting a potential protective role against envenomation. Based on its predicted roles in receptor tyrosine kinase activity and guanine nucleotide exchange, *spri* may be a driver of venom resistance through cell signaling. Finally, with established roles in the regulation of sexual differentiation and sex-specific physiology, *dsx* is likely governing our observed sex-biased nature of venom resistance, although it is not clear whether this is due to venom or resistance mechanisms in general (Zhou *et al.* 2017; Holding *et al.* 2020). Additional roles of *dsx*, including sex-specific synaptic activity, have more recently been identified in *dsx* orthologs in other organisms (Kikkawa and Osumi 2021). Given the number of primary candidate genes identified with known or putative roles in the CNS here, investigating potential connections among these genes, as well as their mechanistic characterizations, is an avenue worthy of exploration in future studies.

Given that the main components of *S. viridis* venom are Ca^{2+} (CAPs) and K^{+} (SLPTXs) ion-channel toxins (Figure 1; Ward *et al.* 2018b), we reasoned that ion-channels would be among the most prominent targets of venom resistance. Somewhat surprisingly, ion channels and/or ion transport were not identified as significantly represented gene ontology (GO) terms (Tables S12 and S14), nor were these genes identified as primary candidates. Although the number of ion channel genes in *D. melanogaster* is reported to be approximately 150–180, corresponding to roughly 1–2% of their total coding genome (Hodge 2009), FlyBase (Thurmond *et al.* 2019) produced a list of 502 *D. melanogaster* "protein-coding ion channel genes" with unique gene identifiers (FBgn numbers). Of these 502 genes, 395 were detected in our full gene list (including all analyses; Table S15), and 36 were detected among our secondary candidate gene list (same significant SNP in E&R time points [FDR < 0.0004], and corresponding significant gene in female XQTL; Figure 6; Table S18). These included some of the most well-characterized *D. melanogaster* ion-channel genes, *Shab* (voltage-gated K^{+}-channel), *SLO2* (calcium-activated K^{+}-channel), and *Orai* (calcium release-activated Ca^{2+}-channel) as well as ionotropic glutamate receptors (*GluRIIA* and *GluRIIB*), nicotinic acetylcholine receptors (*nAChRalpha6* and *nAChRbeta2*), several chemosensory receptor genes, and others with lesser-known functional characterization (Table S18; Thurmond *et al.* 2019). Homologs of these ion channels and receptors are established targets of venom toxins, including those isolated from centipede and other invertebrate venoms (Luo *et al.* 2018; Monge-Fuentes *et al.* 2018; Luo *et al.* 2022; Robinson *et al.* 2022), emphasizing the use of *D. melanogaster* as an applicable model system for venom resistance genetics and also in identifying venom targets with potential therapeutic relevance and translatable applications. Notably, all of our 12 primary candidate genes identified by our analysis have a functional ortholog implicated in human disease (Table S13), including cancer and neuro-degenerative diseases (see Supplementary Results and Discussion), both of which have been documented as human diseases that may benefit from venom-derived therapies (Chen *et al.* 2018; De Souza *et al.* 2018; Fischer and Riedl 2022; Robinson *et al.* 2022).

Understanding venom-mediated coevolution

Our results indicate that the widely-assumed "arms-race" model of coevolution among venomous predator and prey species involving few genes may be vastly oversimplified, as others have suggested (Holding *et al.* 2016). Coevolutionary theory is rich in models and predictions, yet these predictions depend on assumptions about the genetics involved in species interactions, which are completely unknown except for a few remarkably simple cases (Ebert 2018). Furthermore, investigations of mechanisms underlying toxin resistance have often focused on single toxin/resistance gene interactions (Geffeney *et al.* 2002; Feldman *et al.* 2009; Jansa and Voss 2011; Rowe *et al.* 2013; Holding *et al.* 2016; Gibbs *et al.* 2020) and, although some have hinted at the potential of sex-biased selection in prey species (Holding *et al.* 2020), this phenomenon has not been adequately studied and likely affects both fitness and adaptation rate of populations subject to envenomation (Connallon *et al.* 2010) and, reciprocally, imposes selection on the venom itself. Our results provide several concrete patterns that must be incorporated into future attempts at modeling venom-mediated coevolutionary dynamics. First, we have shown that genetic models for the evolution of venom resistance must assume that resistance is based on contributions from hundreds to thousands of loci. Second, we have shown that, in at least one example, a disparity exists between the genetic complexity of venom and venom resistance such that the number of genes involved in resistance is potentially orders of magnitude larger than the complexity of venom. The implied coevolutionary relationships do not consist of simple gene-for-gene interactions, and, should costs of complexity (Orr 2000) exist, they will contribute to venom-mediated coevolutionary dynamics. Finally, the sex-specific response to venom and the drastic difference in resistance genetics between prey sexes introduce a previously unappreciated complication in predicting coevolutionary dynamics. Whether these effects ultimately benefit venomous predators or their prey is unclear and will depend on numerous currently unknown factors (*e.g.*, prey sex ratios and encounter rates). However, as for host-parasite interactions (Duneau and Ebert 2012), evidence for similar effects in natural populations may be found by testing for specialization by venomous predators on a particular prey sex or plastic responses in the handling and envenomation of prey sexes. We have shown that venom resistance can readily evolve and do so without obvious trade-offs, but underlying these simple patterns is a wealth of previously unknown complexity that fundamentally alters how we model coevolutionary processes.

Materials and Methods

Centipedes and venom stock

Adult *Scolopendra viridis* centipedes were collected from the Apalachicola National Forest in Leon County, Florida. Centipedes were housed individually in containers with coconut husk bedding, given water as needed, and fed crickets bi-weekly. Venom was extracted using electrostimulation methods as previously described (Ward *et al.* 2018b). Collected

Table 1. Twelve primary candidate genes and their functions. Genes were identified as significant in E&R generations 12 and 34, as well as in XQTL male and female data sets. Source of function is FlyBase (Thurmond *et al.* 2019) unless otherwise indicated. *Gene also identified in QTL region.

Gene Symbol	FB ID	CHR	POS Start	POS End	Function
baz	FBgn0000163	X	17160006	17200728	Functions in cell polarization pathways in epithelial, neuronal and other cell types
CG11537	FBgn0035400	3L	3128034	3143457	Predicted to be active in membrane and involved in transmembrane transport
*dsx**	FBgn0000504	3R	7924323	7967408	Regulates sexual differentiation
Mctp	FBgn0034389	2R	18761758	18774824	Regulates neuronal synaptic plasticity and neurotransmitter secretion through enabling calcium ion binding
mspo	FBgn0020269	2R	14671396	14713622	Encodes extracellular matrix protein inolved in regulation of myoblast fusion
Ptp61F	FBgn0267487	3L	1342493	1475257	Encodes a non-receptor protein tyrosine phosphatase. A known negative regulator of JAK-STAT, Insulin-like Receptor, EGFR, Pvr, and other kinase-dependent signaling pathways
SKIP	FBgn0051163	3R	22133830	22296126	Regulation of intracellular signal transduction, sensory perception of smell, a potassium channel interacting protein
Spn	FBgn0010905	3L	2505245	2554292	Encodes a protein-phosphotase 1 (PP1) targeting protein that negatively regulates neurexin/neuroligin signaling at the presynaptic zone
spri	FBgn0085443	X	10490069	10585422	Predicted to encode a RAS effector protein, enable receptor tyrosine kinase activity, and guanine nucleotide exchange (GEF)
Svil	FBgn0266696	3L	2377655	2499226	Predicted to be active in actin filament regulation and cytoskeleton organization
tai	FBgn0041092	2L	9166778	9250211	Encodes a steriod hormone receptor coactivator, acts as a transcrption regulator, regulates metabolic processes, and locomotion
X11Lbeta	FBgn0052677	X	10627737	10710947	Predicted to be active in protein localization to the membrane and chemical synaptic transmission

venom was lyophilized and stored at −80°C until later use. For quantitative trait loci (QTL) mapping, venom samples from 20 centipedes were pooled into a single stock of 600 μg as quantified by a NanoDrop 2000 Spectrophotometer (Thermo Fisher Scientific). To ensure consistency of the venom throughout the QTL mapping study, 25 μL aliquots were diluted with sterile PBS based on the determined median lethal dose. A single aliquot was then used for each assay to minimize freeze/thaw events and retain venom function. For the evolve and resequence (E&R) study, a separate venom stock from the same population of 20 centipedes was quantified using a Qubit Fluorometer 1.0 Protein Assay (Thermo Fisher Scientific). The total protein obtained (591 μg) was diluted with sterile PBS and split into several master stock venom aliquots of 1.5 μg/μL, which were then used to prepare 50 μL aliquots of venom based on the determined median lethal dose for the E&R. A single 50 μL aliquot was used for each selection event to minimize freeze/thaw cycles and thereby retain full venom function. For the extreme QTL (XQTL) mapping, venom samples from 31 centipedes were pooled into a single stock of 2.84 mg as quantified by a NanoDrop 2000 Spectrophotometer. To ensure consistency of venom function throughout the XQTL study, 25–50 μL aliquots were diluted with sterile PBS based on the dose required. Aliquots were used a single time to avoid potential loss of function with freeze/thaw cycles.

Centipede genome sequencing and analysis

Genome sequencing

We selected a single female *S. viridis* from the Apalachicola National Forest in Leon County, Florida for genome sequencing. The animal was euthanized by means of prolonged CO_2 exposure and dissected to remove all internal soft tissues. DNA extraction on these tissues, library preparation, and sequencing was performed by the University of Delaware Sequencing and Genotyping Center. PacBio HiFi sequencing was performed on a PacBio Sequel II using two flowcells. The combined output of the two flowcells was 4,810,565 HiFi reads with an N50 of 15.6 Kb and a total of 72.5 Gb of sequence data.

Genome assembly and annotation

HiFi reads were assembled with hifiasm version 0.16.1 (Cheng *et al.* 2021), resulting in an assembly with 2,626 contigs, a contig N50 of 48.5 Mb, and a total length of 2.2 Gb. To assess assembly completeness, we ran BUSCO version 5.2.1 (Simão *et al.* 2015) using the arthropod ortholog set (1,013 sequences). Our hifiasm assembly had 96.4% complete and single copy, 0.6% complete and duplicated, 1.8% fragmented, and 1.2% missing BUSCO loci.

We annotated repeat elements in the hifiasm genome assembly using RepeatModeler (Smit and Hubley 2008) and softmasked the genome with RepeatMasker (Smit *et al.* 2013–2015). We then used funannotate (doi:10.5281/zenodo.1134477) to annotate the softmasked genome. We first used previously published venom-gland RNA-seq data (Ward and Rokyta 2018) from two individuals with NCBI accessions SRR7102114 (C0167) and SRR7102113 (C0169) for gene-prediction training. Adapter and quality trimming was performed with Trim Galore! version 0.6.6 with settings `--length 50 -q 10 -e 0.1 --stringency 1` and CutAdapt version 3.4 (Martin 2011). To facilitate annotation, we generated a consensus *de novo* transcriptome for *S. viridis* using the two RNA-seq data sets above and for *Hemiscolopendra marginata* using previously published data (Nystrom *et al.* 2019) for two individuals with NCBI accessions SRR8188013/SRR8188014 (C0150) and SRR8188011/SRR8188012 (C0162). These consensus assemblies were built following previously published approaches (Ward and Rokyta 2018) and were based on combining initial assemblies generated with DNAStar NGen (version 12.3.1), Extender (Rokyta *et al.* 2012), and Trinity version 2.4.0 (Grabherr *et al.* 2011).

We used these *de novo* assembled consensus coding sequences (CDSs) from *S. viridis* (833 transcripts) and *Hemiscolopendra marginata* (1,008 transcripts) venom-gland transcriptomes, the Arthropoda BUSCO database, and fly as our seed species for gene prediction. Interproscan (Jones *et al.* 2014) was used for functional annotation of predicted gene models. We then filtered the resulting annotations using gffread (Pertea and Pertea 2020) to discard (1) single-exon transcripts, (2) transcripts that did not have CDS features, (3) transcripts that either lacked initial start codons or terminal stop codons or possessed an in-frame stop codon, and (4) genes and their transcripts that had features of pseudogenes. Because venom-gene families in other venomous organisms often occur in large tandem arrays and possess many paralogs (Ye *et al.* 2020; Margres *et al.* 2021) that are difficult for genome annotation packages to fully resolve, we performed additional manual annotation and confirmation of putative venom genes. Venom-gland RNA-seq data for two individuals (C0167 and C0169) were assembled against the genome using the "new Tuxedo" package (Pertea *et al.* 2016). Trimmed venom-gland RNA-seq reads were aligned to the softmasked genome using HiSat2 2.1.0 (Kim *et al.* 2015) to explicitly identify expressed putative toxin genes. Genes were annotated as toxin genes if the gene was expressed in the venom gland and was proteomically confirmed to be present in *S. viridis* venom. Following completion of manual annotation, the trimmed venom-gland RNA-seq reads were again aligned to the softmasked genome using HiSat2 2.1.0 (Kim *et al.* 2015), and transcript expression was quantified using StringTie 1.3.4b (Pertea *et al.* 2015).

We identified 2,439 repeat families with RepeatModeler (Smit and Hubley 2008), and RepeatMasker (Smit *et al.* 2013–2015) masked 60.47% of the genome as repetitive. To verify the efficacy of the built-in duplicate removal strategy for hifiasm, we ran purge_dups version 1.2.5 (Guan *et al.* 2020) on the hifiasm assembly. This reduced the assembly to 848 contigs, a contig N50 of 65.4 Mb, and a total length of 1.8 Gb. We ran RepeatMasker on this reduced genome assembly using the same repeat family library from RepeatModeler. For the smaller genome assembly, RepeatMasker masked 53.50% of the genome as repetitive. These genomes differed in size by 0.446 Gb, and RepeatMasker identified 0.392 Gb (∼88%) of that difference as repetitive. Furthermore, a BUSCO analysis of this reduced assembly showed 96.5% complete and single copy, 0.4% complete and duplicated, 1.8% fragmented, and 1.3% missing BUSCO arthropod loci, nearly identical to the original assembly. We therefore proceeded with the original assembly (before purge_dups) for all analyses. For this final assembly, Funannotate produced 64,280 gene models. The filtering scheme outlined in the above reduced the number of gene models to 40,859. Following manual annotation of putative venom genes, we produced 40,866 gene models, including 98 putative venom genes. To screen for potential contaminants, we ran blobtools version 1.1.1 (Laetsch and Blaxter 2017). Of the 2,626 contigs in our hifiasm assembly, 1,428 matched

to Arthropoda, 1,188 had no hits, four matched Chordata, and six matched to Apicomplexa. We removed the Chordata- and Apicomplexa-matching contigs, which had lengths ranging from 18,264 to 235,724 bp and a combined length of 670,117 bp, from the final assembly after annotation. Our final assembly, after removal of these contigs, consisted of 2,616 contigs with a contig N50 of 48.5 Mb and a total length of 2.2 Gb. Seven of the nonvenom genes were on contigs flagged as contaminants by blobtools and were removed with these contigs in the final assembly.

Venom proteomic composition

For final proteomic confirmation and abundance estimation of venom components, we used previously published shotgun mass-spectrometry venom data (Ward and Rokyta 2018) for the same two individuals used for RNA-seq available through ProteomeXchange under accession PXD009665 with Proteome Discoverer version 2.5 and Scaffold version 5.1.2, using all predicted translations of coding sequences from the annotated genome as the protein database. Peptides and proteins were retained only if they met a threshold of a false discovery rate (FDR) of 1.0% with minimum of at least one unique peptide for a confirmed protein.

Drosophila melanogaster stocks

QTL mapping and E&R

The *Drosophila* Synthetic Population Resource (DSPR) is a multiparental mapping panel with over 1,700 sequenced RILs derived from two recombined, synthetic populations (pA and pB), that were each established from eight inbred founder lines with one line in common between pA and pB (`http://www.flyrils.org/`). A full description of the DSPR and how it can be used to dissect complex traits is provided by King *et al.* (2012b,a). For QTL mapping, 250 pB RILs were maintained in bottles with standard cornmeal-dextrose-yeast media in two incubators held at 25°C on a 12 hour light/dark cycle. Adult flies were transferred into a fresh bottle four days after emergence and cleared from the fresh bottle after four days (populations >100) or seven days (populations <100) to better ensure enough offspring would be available for injections. For the E&R, a genetically mixed population of 835 pB RILs was established using methods previously described (Ng'oma *et al.* 2019) and maintained for approximately 30 generations prior to the start of experimentation.

Extreme QTL (XQTL)

For the extreme QTL (XQTL) experiment an advanced intercrossed population of 37 lines from the *Drosophila* Genetic Reference Panel (DGRP) was used (Fochler *et al.* 2017). These flies were maintained at 25°C on a 12 hour light/dark cycle. To maintain genetic variation, adult flies were selected 3–4 days after after emergence, and 40 males and females were placed into each of 10 different bottles.

Injections

To ensure consistency in life-cycle and metabolic activity, all injections were performed on adult flies 1–3 days after emergence and 1–3 hours after dawn for the flies. Injections were performed following methods previously described (Khalil *et al.* 2015; Ward *et al.* 2018a) using a Drummond Nanoject II Auto-Nanoliter Injector (Drummond Scientific Company) fitted with a glass capillary needle and an injection volume set to 23 nL. Needles were pulled using a Model *p*-87 Flaming/Brown Micropipette Puller (Sutter Instrument Company), and the tips were broken by gently pushing into a Kimwipe tissue. The needle tip opening was then measured using an ocular micrometer on a compound microscope. Only needles measured between 20–40 μm were used for injections. Injections were performed under a stereoscopic microscope with flies anesthetized on a CO_2 plate. Flies were injected in the ventral-lateral portion of the abdomen and placed back into a vial with standard cornmeal-dextrose-yeast media to recover. Vials were positioned on the side to prevent flies from sticking in the media.

QTL mapping in the DSPR

Median lethal dose assays

To obtain a standard venom dose with which to score DSPR RILs, four RILs were selected at random and a full median lethal dose (LD_{50}) assay was performed four times for each of the four RILs using methods previously described (Ward *et al.* 2018a). Flies from each RIL were separated by sex into groups of 10 individuals per vial with standard cornmeal-dextrose-yeast media, and each group of 10 males and 10 females were injected with a single experimental dose. The injected experimental doses were: 1.1, 1.5, 1.9, 2.3, 2.7, 3.1, 3.5, 3.9, and 4.3 ng/mg (venom/fly body weight) based on an average fly weight of 1 mg. Ten flies per sex per RIL were injected with sterile PBS as controls. Because flies would often appear dead and later recover, flies observed at the final 24 hour time point were counted as alive if they exhibited normal behavior and dead if they showed little to no movement when perturbed. LD_{50} values were calculated using the Trimmed Spearman Karber (TSK) method (Hamilton *et al.* 1977) using the *tsk* package in R. Because the goal was to obtain a standard dose to assay all RILs, outliers among replicates for each RIL were identified using the Grubb's outlier test (Grubbs *et al.* 1950) in the *outliers* package in R, and no outliers were detected. The average LD_{50} value for each line was calculated and the resulting average dose among all four lines

(2.99 ng/mg) was used to inject 25 male and 25 female flies from 18 different pB RILs to confirm the calculated LD_{50} dose would achieve an average of 50% death. Because this initial dose resulted in 100% death in a majority of lines tested, the dose was adjusted for male and female flies until the observed death response for each sex exhibited a variable range (15–100%) among 30 RILs. The final doses used to inject 192 RILs to score for venom resistance were 1.87 ng/mg (male dose) and 2.20 ng/mg (female dose).

Phenotypic scoring of RILs

To phenotypically score male and female *D. melanogaster* for venom resistance, 192 RILs from pB of the DSPR were scored by injecting 23 nL of the determined doses (male: 1.87 ng/mg; female: 2.20 ng/mg) of venom and measuring the response (death) to venom injection. For each RIL, 25 males and 25 females were separated into vials and injected with venom following methods described above. A group of 10 males and 10 females per RIL were injected with sterile PBS as controls.

Genetic variance among RILs and broad-sense heritability

Following model fitting recommendations for binomial data by Bolker *et al.* (2009), a generalized linear mixed model (GLMM) was used test whether the observed phenotypic variation among RILs was indicative of genetic variation. The response variable (Y) was the number of alive flies 24 hours post-injection (events) in proportion to the total number of flies injected (trials). The full model, Y ~ Incubator + Date + Incubator*Date + RIL, where Incubator and Date (continuous) were both fixed effects and RIL was a random effect, was implemented using GLIMMIX Procedure in SAS under a binomial distribution with a logit link function. Because different venom doses were used in male and female flies, sexes were analyzed separately. Broad-sense heritability (R^2) was then calculated for binary data as previously described (Davies *et al.* 2015).

QTL peak identification

QTL mapping was performed using methods described by King *et al.* (2012b,a) using the *DSPRqtl* R package (`github.com/egking/DSPRqtl`; `FlyRILs.org`). Because these mapping tools rely on a normal distribution, the response variable (Y) was transformed using the arcsin square root transformation prior to mapping. In the female model for heritability we found significant effects of Incubator, Date, and Incubator*Date, so these terms were included in the mapping model. Normality of the model residuals was confirmed using a combination of the Shapiro-Wilk test for normality (Royston 1982) and a Q-Q-Plot prior to mapping (Figure S2). In the male model for heritability we only found a significant effect of Incubator so this term was included in the male mapping model. However, the residuals of the male data did not fit a normal distribution even after data transformation. We therefore only used the female QTL data for any downstream analyses. A genome scan was performed to regress the eight pB founder genotype probabilities on the transformed response phenotype (female data) at each mapped position. To obtain an appropriate significance threshold, a permutation test was performed using 1,000 permutations of the data with a type I error rate set to $\alpha = 0.05$. Significant QTL were then identified using the DSPRpeaks function with the determined significance threshold and and an LODdrop = 2 for support intervals. QTL with overlapping 95% confidence intervals were considered to be the same peak, and QTL position and confidence interval coordinates were converted to Release 6 of the *D. melanogaster* reference genome assembly on FlyBase (dos Santos *et al.* 2015).

Evolve and resequencing (E&R)

Median lethal dose assays

To obtain a venom dose with which to experimentally evolve venom resistance in *D. melanogaster*, seven replicate LD_{50} assays were performed as described above and previously (Ward *et al.* 2018a) using the genetically mixed *D. melanogater* population (Table S6). In each replicate, 10 males and 10 females per group were separated into vials with standard cornmeal-dextrose and injected with a single venom dose of 0.1, 0.2, 0.3, 0.4, 0.5, 0.6, 0.7, 0.8, 0.9 and 1.0 ng/mg (venom/fly body weight) based on an average fly weight of 1 mg. Ten flies per replicate were injected with sterile PBS as controls. LD_{50} values were calculated using the Trimmed Spearman Karber (TSK) method (Hamilton *et al.* 1977) using the *tsk* package in R (Stone, Brenton R. 2015). In the event that one or more individuals died in the control group, the assay was not included in the LD_{50} calculation of median, mean, or comparisons to other replicates. In the event where the recommended trim using the TSK method was greater than 0.3 (recommended trim values range from 0.0–0.5), the assay was not included in the LD_{50} calculation of median, mean, or comparisons to other replicates as higher trim values may yield less reliable LD_{50} calculations. To test for outliers among replicates, the Grubb's outlier test (Grubbs *et al.* 1950) was performed using the *outliers* package in R. The resulting TSK median dose value among replicates of the mixed population was 0.47 ng/mg and this dose was used to select for venom resistance over the first 12 generations of selection. Based on the phenotypic response to selection after the first 12 generations, a full median lethal dose assay was completed to assess differences among control and venom-injected replicates. Because the TSK method of LD_{50} calculation does not allow for statistical

comparison of values (Schenker and Gentleman 2001), an independent dose response model (DRM) was used to calculate a median effective dose (ED_{50}) using the *drc* package in R following methods previously described (Margres *et al.* 2017; Ward *et al.* 2018a). This method also allows for adjustments to the model parameters to ensure the calculated ED_{50} value represents an appropriate fit for the data (a lower standard error indicates a better model fit) and does not suffer from the same trim constraints as the TSK method. Therefore, the resulting ED_{50} values from the DRM model were used for visualization and comparison among replicates. To determine whether the venom-injected replicates were more resistant (*i.e.,* had a significantly higher ED_{50} value) in comparison to the control replicates (non-injected and PBS-injected), the `comped` function in R was used to perform Wheeler's ratio test (Wheeler *et al.* 1983) between the most resistant control replicate to the least resistant venom-injected replicate. Based on this ratio test, ED_{50} values are considered significantly different if the confidence intervals for the ratios do not contain 1. An unpaired *t*-test was also used to determine if the mean DRM ED_{50} values for the control and venom-injected replicates were significantly different (Table S6). Because the venom-injected and control replicates were not significantly different from each other at this point, selection continued using the new TSK calculated median LD_{50} value among all venom-injected and control replicates of 0.55 ng/mg. After 18 months and 34 total generations of selection for venom resistance, a final median lethal dose assay was completed on each venom-injected and control replicate to assess whether the venom-injected replicates were significantly more resistant to venom compared to PBS-injected and non-injected controls.

Experimental evolution

Due to labor-intensive nature of the selection events (manually injecting individual flies), we first determined the number of individual *D. melanogaster* that could be injected within an established time frame, such that injections could occur at the same time of day for the flies to ensure consistency of life-cycle and metabolic activity (see Methods, Injections). With this in mind, 500 flies could be injected within the 2 hour time frame. We then prioritized experimental design parameters based on recommendations for E&R studies using *D. melanogaster* (Kofler and Schlötterer 2014; Kessner and Novembre 2015; Schlötterer *et al.* 2015). We therefore established a genetically diverse starting population (see Methods, *Drosophila melanogaster* stocks, *QTL mapping and E&R*), performed selection events every other generation (to allow for population size recovery and recombination), used four venom-injected replicates (more than the recommended three, and favored over an increase in population size), and continued selection for 34 generations (more than recommended). Combined with simulating our experimental design to identify candidate SNPs (see Methods, Evolve and resequencing, *Identifying candidate SNPs*), we reasoned these parameters provided sufficient power in reducing effects of drift and detecting true positive targets of venom resistance in our E&R study. The mixed *D. melanogaster* population was used to establish eight replicate populations of approximately 2,000 randomly selected flies each. Of the eight replicate populations, four were venom-injected (V1, V2, V3, V4), two were PBS-injected controls (PC1, PC2), and two were non-injected controls (C1, C2). Populations were distributed in two incubators (Inc. 1: PC1, C1, V1, V3; Inc. 2: C2, PC2, V2, V4) held at 25°C on a 12 hour light/dark cycle and fed standard cornmeal-dextrose-yeast media. At each selection event, 500 flies (250 males and 250 females, randomly selected from the appropriate population replicate) were injected with 23 nL of 0.47 ng/mg *S. viridis* venom. Flies were injected in groups of 25 to minimized CO_2 exposure. After 24 hours, surviving flies were recombined into fresh bottles in approximately equal sex-ratios ranging from 50–100 flies per bottle. Adult flies were cleared after seven days and preserved for sequencing in a 1.5 mL cryo-tube with 95% ethanol at -80°C. Four days after emergence, the successive generation was released into a population cage equipped with six bottles of fresh media. After three days, the six bottles of media seeded with eggs were collected, and adults emerging from these bottles were subjected to the next round of selection such that selection occurred every other generation to allow for population size recovery and reduce effects of linkage disequilibrium by increasing recombination between selection events (Terhorst *et al.* 2015). In some cases, an extra generation was required for population size recovery (Table S7). The PBS-injected control replicates followed the same procedure but were injected with 23 nL of sterile PBS rather than venom. The non-injected control replicates also followed the same procedure, but rather than being injected, 1–3 day emerged adults were mixed and redistributed into fresh bottles to mimic the bottleneck effect of the injected replicates. Because the phenotypic response of the venom-injected replicates decreased from an average of 55% to 12% after six months of selection (approximately 7 selection events and 12 generations per replicate, Figure 4), a median lethal dose assay was performed (using methods described above) on each of the venom-injected, PBS-injected, and non-injected replicates to determine if the venom-injected replicates had significantly increased resistance to venom in comparison to the controls. No significant difference was found among control and venom-injected replicates. The median LD_{50}

value, however, increased to 0.55 ng/mg. Selection for venom resistance continued using 0.55 ng/mg *S. viridis* venom until reaching 18 months of selection (approximately 15 selection events and 34 generations per replicate). A final median lethal dose assay was performed on each venom-injected, PBS-injected, and non-injected replicate to assess the level of increased venom resistance in the venom-injected replicates in comparison to the control replicates (Table S6). Effective population size (N_e) of each replicate was calculated using poolSeq (Taus *et al.* 2017) with allele frequencies obtained from sequencing data (Table S9), as well as by calculating the harmonic mean (Pertoldi *et al.* 2007) using phenotypic data for each selection event (Tables S7 and S10).

Measurement of life history traits

Throughout the course of the experimental evolution study, multiple life-history trait measurements were recorded on each of the venom-injected and PBS-injected replicates to assess potential costs of resistance (Table S8). To determine if the measured life-history traits were affected by selection for venom resistance, each trait was analyzed as the response over time (selection) in a model that included a both a linear (selection) and quadratic (selection^2) time coefficient and tested for an interaction effect of group (PBS-injected versus venom-injected) using the `lm` function in R. **Weight:** At each selection event a group of 25 male and 25 female *D. melanogaster* were weighed to the nearest mg to track the average fly weight for each replicate over time. **Emergence Time:** For our purposes, emergence time refers to the emergence of offspring of injected survivors measured as the number of days from the initial day of mating/ovipositing on fresh media to the date of observed emergence. **Offspring:** As mentioned above, flies that survived injections (either venom-injected or PBS-injected) were recombined into fresh bottles and cleared seven days later. Bottles were then monitored for emergence of the next generation by checking bottles daily for developed pupae. On the day of initial observation of emerged flies (measured as emergence time), photographs were taken of each side (four) of each bottle (1–5 bottles per replicate depending on the number of survivors). The observed pupae were then counted from the photographs by two independent observers. Offspring was then measured as the average pupae count of the two observers, divided by the number of parental females.

Whole-genome sequencing, mapping, and SNP identification

Whole-genome sequencing was performed on each of the ancestral (1 population), mid-point (8 populations), and final (8 populations) time points of the experimental evolution study using methods recommended by Schlötterer *et al.* (2015). The ancestral population refers to the starting mixed population prior to any experimentation. The mid-point populations refer to the four venom-injected, two PBS-injected, and two non-injected replicates at generation 12–14, after approximately six months and seven selection events (referred to as generation 12 throughout the manuscript). The final populations refer to the four venom-injected, two PBS-injected, and two non-injected replicates at generation 33–35 after 18 months and 15 selection events (referred to as generation 34 throughout the manuscript). A group of 50–70 *D. melanogaster* individuals in equal sex ratios were pooled per population. DNA extractions and library preparations were performed by the Florida State University Molecular Cloning Facility. To extract high-molecular weight DNA for sequencing, flies from each population pool were homogenized in BL Buffer (Omega BioTek, Inc.) using a motorized pestle system with sterile, single-use pestles, and DNA was extracted using the E.Z.N.A.® Tissue DNA Kit (Omega Bio-Tek, Inc.) following manufacturer's instructions. High-molecular weight DNA was then sheared to approximately 500 base pairs using a Covaris® ME220 Focused-ultrasonicator (Covaris, Inc.). Sheared DNA was quality checked using a High Sensitivity D1000 ScreenTape® (Agilent Technologies, Inc.). DNA libraries were then prepared using the NEBNext® Ultra™ II DNA Library Prep Kit for Illumina® (New England BioLabs, Inc.) with AMPure XP purification beads (Beckman Coulter, Inc.) and NEBNext® Multiplex Oligos for Illumina® on a Biomek 4000 Automated Liquid Handler (Beckman Coulter, Inc.), such that each population library was uniquely indexed. Individual libraries were quality checked using a High Sensitivity D1000 ScreenTape® and KAPA qPCR to determine amplifiable concentration. Libraries were then pooled and quality checked using a High Sensitivity D1000 ScreenTape® and qPCR to obtain a final amplifiable concentration of approximately 5 nM for sequencing. Sequencing was performed by the Florida State University College of Medicine Translational Science Lab using 150 paired-end chemistry on an Illumina® NovaSeq 6000. Trim Galore! v0.6.0 and FastQC v0.4.4 were used for quality trimming and adapter removal of raw reads, retaining a minimum sequence length of 50 and quality threshold of 10. Trimmed reads were aligned to the *D. melanogaster* genome (release 6.29) mapping algorithm BWA-MEM (Li 2013) in BWA (version 0.7.17-r1188; Li and Durbin 2009). We filtered alignment files for reads mapped in proper read pairs at a threshold mapping quality of 20 (samtools view -q 20 -b), and converted the SAM files to BAM format using SAMtools (Li *et al.* 2009; Li 2011). We used Picard Tools (version 2.22) to assign desired read groups to the headerless BAM files in the output (AddOrReplaceReadGroups) and remove potential PCR duplicates (MarkDuplicates). From

this point, we used GATK (version 3.81) (McKenna *et al.* 2010; DePristo *et al.* 2011) based on the Best Practices Pipeline (Van der Auwera *et al.* 2013), to (1) call haplotypes for the 8 founder lines of the DSPR (King *et al.* 2012a,b) using the HaplotypeCaller (Poplin *et al.* 2017) in GVCF mode, (2) call variants using the GenotypeGVCF module, and (3) filter for variant quality using the VariantFiltration module (clusterWindowSize 10, QUAL > 30.0, QD > 5.0, FS > 60.0). We annotated quality-filtered VCF using the *D. melanogaster* genome annotation file, BDGP6.86, which we parsed with a custom script to generate a table of variants. SNPs were limited to mapped regions (2L, 2R, 3L, 3R, 4, X, Y) and the minimum minor allele count was 2. Indels and SNPs within 5bp of an indel were excluded. Read depth distributions were determined for each sample using samtools depth (Li *et al.* 2009; Li 2011), and the top and bottom 1% of SNPs were trimmed based on the samples with the highest and lowest distributions such that SNPs were retained with read depths > 14 and < 161. This set of quality-filtered SNPs (1,498,163 SNPs) are consistent with the set of previously identified high confidence SNPs in the DSPR founder lines (∼66% of SNPs called are in this high confidence set (King *et al.* 2012b)).

Identifying candidate SNPs

To determine significant allele frequency differences between control and venom-injected replicates for each time point, the Cochran-Mantel-Haenszel (CMH) test was implemented in PoPoolation2 (Kofler *et al.* 2011) which has been shown to be one of the best methods for detecting selected SNPs in E&R data (Vlachos *et al.* 2019). Because the CMH test requires pairing of selection to control replicates, each selected and control replicate were paired within incubator and both possible pairs per incubator were tested, resulting in two CMH tests per generation. Significance thresholds were determined by simulating our experimental design using MimicEE2 (Vlachos and Kofler 2018), in which forces of drift, selection, and recombination were validated. Our simulated starting population was formed by mixing all 835 pB RIL haplotypes for 30 generations under neutral selection and confirming that the heterozygosity of the resulting simulated population ($H = 0.205$) was comparable to our experimental starting population ($H = 0.213$). To mimic our full experimental design under neutral selection, the simulated starting population was used to simulate eight populations (representing 2 non-injected, 2 PBS-injected, and 4 venom-injected replicates) with alternating population sizes of 2000 and 500 every other generation and collecting snapshots at generation 12 and 34, performed in triplicate. To mimic empirical sequencing conditions, PoolSeq (Taus *et al.* 2017) was used to sample simulated replicates such that each replicate represented a random sample of 70 individuals, and coverage was drawn from a random distribution around the average sequencing depth of the empirical data replicates (average coverage = 88). For each triplicate simulation representing generation 12 and 34, the CMH test was used to pair and cross-pair populations randomly designated to represent venom and control replicates, resulting in two CMH tests per generation per simulated replicate. Following methods previously described (Orozco-Terwengel *et al.* 2012), we found the *p*-value associated with a quantile of 0.001 (or 99.99 percentile) in each simulated replicate. The largest of these *p*-values for each time point was used as the significance threshold in our empirical data (Generation 12: $p = 4.11 \times 10^{-6}$, Generation 34: $p = 1.01 \times 10^{-8}$; Table S4). Significant SNPs were then filtered by taking the intersect of the two cross-paired CMH tests per time point, resulting in a final set of SNPs per time point with consistent differences between venom-injected and control (either non-injected or PBS-injected) replicates. After identifying significant SNPs for each simulated generation 12 and 34, common significant SNPs to both generations were also determined (Generation 1234; Table S4). The false discovery rate (FDR) for significant SNPs in our empirical data was calculated by dividing the average number of significant SNPs from simulated replicates (Generation 12 = 849, Generation 34 = 946, Generation 1234 = 2.3) by the number of significant SNPs in empirical data (Generation 12 = 38,585, Generation 34 = 66,506, Generation 1234 = 5,864), resulting in an FDR > 0.0220, > 0.0142, and > 0.0004 for Generation 12, Generation 34, and those common to Generations 12 and 34 (Generation 1234) SNPs, respectively (Table S4). Manhattan plots of the simulated data were generated for visual comparison to empirical data (Figure S4).

Inferring selected haplotypes

We followed a similar haplotype estimation method as described by Burke *et al.* (2014). First, we filtered our set of SNPs to consist only of those shared between the SNPs previously identified in the DSPR founders and those in our dataset. This set consisted of ∼1 million SNPs (1,025,372). In short, we then used an optimization approach to identify, for a given window of allele frequencies in a given sample, the combination of founder haplotype frequencies most likely to produce that observed set of allele frequencies. We used a window size of 3,000 SNPs with a step size of 50 SNPs. Prior simulations using the DSPR RILs show a window size of 3,000 SNPs gives the best accuracy. In addition, a smaller window size of 200 SNPs produced similar results, demonstrating that our haplotype inference is stable over a reasonable range of window sizes, which is

also supported by previous simulations. At each focal position, we used the `optim` function in R to identify the set of founder haplotype frequencies that minimize the following quantity (similar to a sum of squares):

$$\sum_{i=1}^{3000} \sqrt{C_i} \cdot (MAF_i - \sum_{j=1}^{8} (f_{ij} \cdot h_{ij})^2) + (100 \cdot ((\sum_{j=1}^{8} h_{ij}) - 1)^2)$$

where C_i is the sequence coverage at the ith SNP in the window, MAF_i is the alternative allele frequency at the ith SNP, f_{ij} is the allelic state of the jth founder at the ith SNP (0/1), and h_{ij} is the haplotype frequency of the jth founder at the ith SNP. The second part of the above equation serves as a penalty when the sum of the 8 founder haplotype frequencies exceeds 1 to prevent this occurrence. In addition, each individual haplotype frequency is bounded by 0 and 0.95. This results in an estimated set of 8 haplotype frequencies for each window across the genome.

To identify regions with consistent changes in haplotype frequencies in response to venom injection, we performed a repeated measures ANOVA with arcsine square root transformed haplotype frequency predicted by haplotype id, treatment, and their interaction, with incubator as a grouping variable as follows:

$$H_{\mathrm{f}} \sim H_{\mathrm{ID}} + T + H_{\mathrm{ID}} \cdot T + (1|I)$$

where H_{f} is haplotype frequency, H_{ID} is haplotype ID, T is treatment, and I is incubator. A significant interaction term indicates a position in which the venom-treated and control replicates differ significantly in the set of 8 haplotype frequencies. For this model, we grouped all controls together to increase our power to detect consistent effects between the venom and control replicates. We fit this model at each of our windows in which we estimated haplotype frequencies across the genome. To account for these multiple comparisons, we used the FDR correction for multiple comparisons in R (Benjamini and Hochberg 1995) to obtain adjusted p-values.

All scripts and a step-by-step protocol to reproduce these analyses are provided here `https://github.com/ECKingLab/Venom_ResEvol`.

Extreme QTL mapping (XQTL)

Median lethal dose assays

Lethal dose assays were performed as described above. However, to capture the most extreme phenotype to venom resistance, we injected flies with a venom dose corresponding to 80% lethality rather than 50%. An independent dose response model (DRM) was used to calculate a 80% effective dose (ED_{80}) using the *drc* package in R following methods previously described (Margres *et al.* 2017; Ward *et al.* 2018a). The ED_{80} dose was calculated for males and females independently. Adjustments to the doses were made to ensure that 10–20% of the flies injected survived for sequencing. The ED_{80} used for males was 3.1 ng/mg and 7.5 ng/mg was used for the females.

Extreme QTL mapping experiment

For the XQTL analysis we followed the design laid out previously (Fochler *et al.* 2017; Anholt and Mackay 2018). 600 flies were randomly selected and injected with the ED_{80} as calculated above. Surviving flies (between 10–20%) were collected in ethanol and saved for sequencing. At each injection event, 100 flies from the base population were selected at random and saved for genetic comparison to those that survived venom injection. XQTL experiments were performed in duplicate for each sex, with 112 and 135 male survivors, and 112 and 124 female survivors of venom injection in each replicate.

Whole-genome sequencing, mapping, and SNP identification

For each injection event (two all-male and two all-female), all venom injected survivors (112 and 135 for each male replicate, and 112 and 124 for each female replicate) were pooled and sequenced, and a pool of 100 flies from the base population was sequenced as a control. Whole-genome sequencing and data analysis was performed as described above (see Methods, Evolve and resequencing, *Whole-genome sequencing, mapping, and SNP identification*), retaining read depths > 3 and < 152 and > 5 and < 238 for males and females, respectively. After all of the quality filtering for the SNPs, 1,109,591 and 1,214,086 SNPs were retained for the males and females, respectively.

Identifying candidate SNPs

Candidate SNPs were identified using the CMH test as described above. The male and female data sets were run separately and their p-values were adjusted using the FDR correction. SNPs were considered significant if their adjusted p-value was less than 0.05. This resulted in 70 and 19,862 significant SNPs for males and females, respectively.

Identifying candidate genes

Genes were identified as significant in the E&R if they contained a significant SNP (see E&R Identifying candidate SNPs). Because the results of the E&R analysis revealed a genome-wide response with a large number of significant SNPs and genes for each sequenced time point (generation 12 and 34), we used the significant E&R SNPs as a basis to identify candidate genes within the significant QTL region (identified using females from 192 DSPR RILs) and within significant haplotype blocks (identified by inferring selected DSPR founder haplptypes). This resulted in a set of significant SNPs for each generation within the QTL and haplotype block regions. We then used Gowinda (Kofler and Schlötterer 2012) to identify candidate genes in these regions, as well as identify significant GO terms (see below). Gowinda was run in gene mode with 100,000 simulations and included regulatory regions

2000bp up and downstream of each gene. The GO Association file was downloaded from FuncAssociate 3.0 (Berriz *et al.* 2003) on 6/4/2020. Additionally, because the E&R (DSPR mixed population) and XQTL (DGRP mixed population) analyses are fully independent and both resulted in a genome-wide response, we considered genes containing a significant SNP(s) in both the E&R (where the same SNP was identified as significant at both time points) and the XQTL as candidate genes. Although we identified several gene lists with varying overlap among analyses (Table S5), we ultimately focused our attention on areas of overlap among the most independent forms of analyses (E&R and XQTL) where we found consistency between the two time points (Figure 6). We identified 12 candidate genes with common significant SNPs at both time points of the E&R that were also present in both sexes of the XQTL. We considered these our primary candidate genes. We also identified 739 candidate genes with common significant SNPs at both time points of the E&R that were also present in the female XQTL data set, which we considered our secondary candidate genes. A complete gene list of all genes identified by analyses is provided in supplementary table S15.

Network Analysis

We conducted a network analysis using the *D. melanogaster* FlyBase database (Thurmond *et al.* 2019) in the esyN portal (Bean *et al.* 2014) to search for known genetic and physical interactions among candidate genes of interest. We mapped a network of the 12 primary candidate genes and their first-degree interactions (Figure S8).

Gene ontology (GO)

As described above, we used Gowinda (Kofler and Schlötterer 2012) to perform GO analysis of all significant genes identified in each E&R generation, within the QTL and haplotype block regions and for the male and female XQTL data. Because GO tests are inherently biased towards a high false-positive rate, we identified GO terms as significant if the false discovery rate (FDR) adjusted p-value was less than 0.05. All genes present in the significant GO terms were compiled and organized by their unique FlyBase (Thurmond *et al.* 2019) gene identification number (FBgn#). The unique FBgn#s were converted to their respective gene symbols and searched through the FlyBase gene database using FlyBase ID validator and BioTools.fr to identify genes with alleles used as a model for human diseases (Tables S12, S14).

Supplementary Material

Supplementary material is available at Molecular Biology and Evolution online.

Conflict of interest

The authors declare no conflicts of interest.

Acknowledgments

This material is based upon work supported by the National Science Foundation Graduate Research Fellowship Program under Grant No. 1449440 to M.J.W. Any opinions, findings, and conclusions or recommendations expressed in this material are those of the authors and do not necessarily reflect the views of the National Science Foundation. Funding for this work was provided by the National Science Foundation (NSF DEB 1145978 and NSF DEB 1638902 to D.R.R, NSF DEB 1822417 to C.L.P., and NSF DEB 2027446 to M.J.M.), the Florida State University Council on Research and Creativity, the Margaret Menzel Fellowship, the Ben and Karen Thrower Scholarship, and the Lamar and Edith Trott Scholarship. Computation for this work was performed on the high performance computing infrastructure provided by Research Computing Support Services and in part by the National Science Foundation under grant number CNS-1429294 at the University of Missouri, Columbia MO. DOI: `https://doi.org/10.32469/10355/69802`.

Data availability

***Drosophila melanogaster* sequencing:** The genomic sequencing data are available through NCBI under BioProject PRJNA340270. The E&R data is under BioSample SAMN54570816 (SRA accessions SRR36788783–SRR36788799). The XQTL female data is under SAMN54577700 (SRR accessions SRR36804991–SRR36804994). The XQTL male data is under SAMN54577701 (SRR accessions SRR36804987–SRR36804990).

***Scolopendra viridis* genome:** The raw PacBio HiFi reads are available through NCBI under BioProject PRJNA947954 and SRA accession SRR23948554. The assembled genome is available in the NCBI Whole Genome Shotgun (WGS) database under accession JBAMJC000000000.

References

Anholt RR, Mackay TF. The road less traveled: from genotype to phenotype in flies and humans. *Mammalian Genome*. 2018:**29**(1-2):5–23. https://doi.org/10.1007/s00335-017-9722-7.

Baeg GH, Zhou R, Perrimon N. Genome-wide RNAi analysis of JAK/STAT signaling components in *Drosophila*. *Genes and Development*. 2005:**19**(16):1861–1870. https://doi.org/10.1101/gad.1320705.

Barghi N, Hermisson J, Schlötterer C. Polygenic adaptation: a unifying framework to understand positive selection. *Nature Reviews Genetics*. 2020: **21**(12):769–781. https://doi.org/10.1038/s41576-020-0250-z.

Barghi N, Tobler R, Nolte V, Jakšić AM, Mallard F, Otte KA, Dolezal M, Taus T, Kofler R, Schlötterer C. Genetic redundancy fuels polygenic adaptation in *Drosophila*. *PLoS Biology*. 2019:**17**(2):e3000128. https://doi.org/10.1371/journal.pbio.3000128.

Bean DM, Heimbach J, Ficorella L, Micklem G, Oliver SG, Favrin G. esyN: network building, sharing and publishing. *PloS One*. 2014:**9**(9):e106035. https://doi.org/10.1371/journal.pone.0204058.

Benjamini Y, Hochberg Y. Controlling the false discovery rate: a practical and powerful approach to multiple testing. *Journal of the Royal Statistical Society: Series B (Methodological)*. 1995: **57**(1):289–300. https://doi.org/10.1111/j.2517-6161.1995.tb02031.x.

Berriz GF, King OD, Bryant B, Sander C, Roth FP. Characterizing gene sets with FuncAssociate. *Bioinformatics*. 2003:**19**(18):2502–2504. https://doi.org/10.1093/bioinformatics/btg363.

Bolker BM, Brooks ME, Clark CJ, Geange SW, Poulsen JR, Stevens MHH, White JSS. Generalized linear mixed models: a practical guide for ecology and evolution. *Trends in Ecology and Evolution*. 2009:**24**(3):127–135. https://doi.org/10.1016/j.tree.2008.10.008.

Brodie III ED, Brodie Jr ED. Predator-prey arms races: asymmetrical selection on predators and prey may be reduced when prey are dangerous. *Bioscience*. 1999:**49**(7):557–568. https://doi.org/10.2307/1313476.

Burke MK, King EG, Shahrestani P, Rose MR, Long AD. Genome-wide association study of extreme longevity in *Drosophila melanogaster*. *Genome Biology and Evolution*. 2014:**6**(1):1–11. https://doi.org/10.1093/gbe/evt180.

Byun PK, Zhang C, Yao B, Wardwell-Ozgo J, Terry D, Jin P, Moberg K. The Taiman transcriptional coactivator engages Toll signals to promote apoptosis and intertissue invasion in *Drosophila*. *Current Biology*. 2019:**29**(17):2790–2800. https://doi.org/10.1016/j.cub.2019.07.012.

Chen N, Xu S, Zhang Y, Wang F. Animal protein toxins: origins and therapeutic applications. *Biophysics Reports*. 2018:**4**(5):233–242. https://doi.org/10.1007/s41048-018-0067-x.

Cheng H, Concepcion GT, Feng X, Zhang H, Li H. Haplotype-resolved de novo assembly using phased assembly graphs with hifiasm. *Nature Methods*. 2021:**18**:170–175. https://doi.org/10.1038/s41592-020-01056-5.

Clement DT, Gallinson DG, Hamede RK, Jones ME, Margres MJ, McCallum H, Storfer A. Coevolution promotes the coexistence of Tasmanian devils and a fatal, transmissible cancer. *Evolution*. 2025:**79**:100–118. https://doi.org/10.1093/evolut/qpae143.

Connallon T, Cox RM, Calsbeek R. Fitness consequences of sex-specific selection. *Evolution*. 2010:**64**(6):1671–1682. https://doi.org/10.1111/j.1558-5646.2009.00934.x.

Cox RM, Calsbeek R. Sexually antagonistic selection, sexual dimorphism, and the resolution of intralocus sexual conflict. *The American Naturalist*. 2009: **173**(2):176–187. https://doi.org/10.1086/595841.

Dal Peraro M, Van Der Goot FG. Pore-forming toxins: ancient, but never really out of fashion. *Nature Reviews Microbiology*. 2016: **14**(2):77. https://doi.org/10.1038/nrmicro.2015.3.

Davies SW, Scarpino SV, Pongwarin T, Scott J, Matz MV. Estimating trait heritability in highly fecund species. *G3: Genes, Genomes, Genetics*. 2015:**5**(12):2639–2645. https://doi.org/10.1534/g3.115.020701.

Davis MM, Engström Y. Immune response in the barrier epithelia: lessons from the fruit fly *Drosophila melanogaster*. *Journal of Innate Immunity*. 2012:**4**(3):273–283. https://doi.org/10.1159/000332947.

Dawkins R. *The Extended Phenotype: The Long Reach of the Gene*. Oxford University Press. 2016.

De Souza JM, Goncalves BD, Gomez MV, Vieira LB, Ribeiro FM. Animal toxins as therapeutic tools to treat neurodegenerative diseases. *Frontiers in pharmacology*. 2018:**9**:145. https://doi.org/10.3389/fphar.2018.00145.

Denell R, Keppy D. The nature of genetic recombination near the third chromosome centromere of *Drosophila melanogaster*. *Genetics*. 1979:**93**(1):117–130. https://doi.org/10.1093/genetics/93.1.117.

DePristo MA, Banks E, Poplin R, Garimella KV, Maguire JR, Hartl C, Philippakis AA, Del Angel G, Rivas MA, Hanna M, *et al.* A framework for variation discovery and genotyping using next-generation DNA sequencing data. *Nature Genetics*. 2011:**43**(5):491. https://doi.org/10.1038/ng.806.

dos Santos G, Schroeder AJ, Goodman JL, Strelets VB, Crosby MA, Thurmond J, Emmert DB, Gelbart WM, Consortium F. Flybase: introduction of the *Drosophila melanogaster* release 6 reference genome assembly and large-scale migration of genome annotations. *Nucleic Acids Research*. 2015:**43**(D1):D690–D697. https://doi.org/10.1093/nar/gku1099.

Du TY, Hall SR, Chung F, Kurdyukov S, Crittenden E, Patel K, Dawson CA, Westhorpe AP, Bartlett KE, Rasmussen SA, *et al.* Molecular dissection of cobra venom highlights heparinoids as an antidote for spitting cobra envenoming. *Science Translational Medicine*. 2024:**16**:eadk4802. https://doi.org/10.1126/scitranslmed.adk4802.

Duneau D, Ebert D. Host sexual dimorphism and parasite adaptation. *PLOS Biology*. 2012:**10**:e1001271. https://doi.org/10.1371/journal.pbio.1001271.

Duneau D, Luijckx P, Ruder LF, Ebert D. Sex-specific effects of a parasite evolving in a female-biased host population. *BMC Biology*. 2012:**10**:104. https://doi.org/10.1186/1741-7007-10-104.

Ebert D. Open questions: what are the genes underlying antagonistic coevolution? *BMC Biology*. 2018:**16**:114. https://doi.org/10.1186/s12915-018-0583-7.

Ellsworth SA, Rautsaw RM, Ward MJ, Holding ML, Rokyta DR. Selection across the three-dimensional structure of venom proteins from North American scolopendromorph centipedes. *Journal of Molecular Evolution*. 2024:**92**:505–524. https://doi.org/10.1007/s00239-024-10191-y.

Feldman CR, Brodie Jr ED, Brodie III ED, Pfrender ME. The evolutionary origins of beneficial alleles during the repeated adaptation of garter snakes to deadly prey. *Proceedings of the National Academy of Sciences*. 2009:**106**(32):13415–13420. https://doi.org/10.1073/pnas.0901224106.

Fischer T, Riedl R. Paracelsus' legacy in the faunal realm: drugs deriving from animal toxins. *Drug Discovery Today*. 2022:**27**(2):567–575. https://doi.org/10.1016/j.drudis.2021.10.003.

Fisher RA. *The Genetical Theory of Natural Selection*. Oxford University Press, Oxford (UK). 1930.

Fochler S, Morozova TV, Davis MR, Gearhart AW, Huang W, Mackay TF, Anholt RR. Genetics of alcohol consumption in *Drosophila melanogaster*. *Genes, Brain and Behavior*. 2017:**16**(7):675–685. https://doi.org/10.1111/gbb.12399.

Foerster K, Coulson T, Sheldon BC, Pemberton JM, Clutton-Brock TH, Kruuk LE. Sexually antagonistic genetic variation for fitness in red deer. *Nature*. 2007:**447**(7148):1107–1110.

Fry JD. The genomic location of sexually antagonistic variation: some cautionary comments. *Evolution*. 2010:**64**(5):1510–1516.

Gallinson DG, Kozakiewicz CP, Rautsaw RM, Beer MA, Ruiz-Aravena M, Comte S, Hamilton DG, Kerlin DH, McCallum HI, Hamede R, *et al.* Intergenomic signatures of coevolution between Tasmanian devils and an infectious cancer. *Proceedings of the National Academy of Sciences*. 2024:**121**:e2307780121. https://doi.org/10.1073/pnas.2307780121.

Geffeney S, Brodie Jr ED, Rubin PC, Brodie III ED. Mechanisms of adaptation in a predator-prey arms race: TTX-resistant sodium channels. *Science*. 2002:**297**:1336–1339. https://doi.org/10.1126/science.1074310.

Gibbs HL, Sanz L, Pérez A, Ochoa A, Hassinger AT, Holding ML, Calvete JJ. The molecular basis of venom resistance in a rattlesnake-squirrel predator-prey system. *Molecular Ecology*. 2020:**29**(15):2871–2888. https://doi.org/10.1111/mec.15529.

Gipson SAY, Hall MD. The evolution of sexual dimorphism and its potential impact on host–pathogen coevolution. *Evolution*. 2016:**70**:959–968. https://doi.org/10.1111/evo.12922.

Grabherr MG, Haas BJ, Yassour M, Levin JZ, Thompson DA, Amit I, Adiconis X, Fan L, Raychowdhury R, Zeng Q, *et al.* Full-length transcriptome assembly from RNA-Seq data without a reference genome. *Nature Biotechnology*. 2011:**29**(7):644–652. https://doi.org/10.1038/nbt.1883.

Grubbs FE, *et al.* Sample criteria for testing outlying observations. *The Annals of Mathematical Statistics*. 1950:**21**(1):27–58. https://doi.org/10.1214/aoms/1177729885.

Guan D, McCarthy SA, Wood J, Howe K, Wang Y, Durbin R. Identifying and removing haplotypic duplication in primary genome assemblies. *Bioinformatics*. 2020:**36**(9):2896–2898. https://doi.org/10.1093/bioinformatics/btaa025.

Hamilton MA, Russo RC, Thurston RV. Trimmed Spearman-Karber method for estimating median lethal concentrations in toxicity bioassays. *Environmental Science and Technology*. 1977:**11**(7):714–719. https://doi.org/10.1021/es60130a004.

Hawkes M, Gamble C, Turner E, Carey M, Wedell N, Hosken D. Intralocus sexual conflict and insecticide resistance. *Proceedings of the Royal Society B: Biological Sciences*. 2016:**283**(1843):20161429. https://doi.org/10.1098/rspb.2016.1429.

Hodge JJ. Ion channels to inactivate neurons in drosophila. *Frontiers in Molecular Neuroscience*. 2009:**2**:796. https://doi.org/10.3389/neuro.02.013.2009.

Hogan MP, Holding ML, Nystrom GS, Colston TJ, Bartlett DA, Mason AJ, Ellsworth SA, Rautsaw RM, Lawrence KC, Strickland JL, *et al.* The genetic regulatory architecture and epigenomic basis for age-related changes in rattlesnake venom. *Proceedings of the National Academy of Sciences*. 2024:**121**:e2313440121. https://doi.org/10.1073/pnas.2313440121.

Holding ML, Drabeck DH, Jansa SA, Gibbs HL. Venom resistance as a model for understanding the molecular basis of complex coevolutionary adaptations. *Integrative and Comparative Biology*. 2016:**56**(5):1032–1043. https://doi.org/10.1093/icb/icw082.

Holding ML, Putman BJ, Kong LM, Smith JE, Clark RW. Physiological stress integrates resistance to rattlesnake venom and the onset of risky foraging in california ground squirrels. *Toxins*. 2020:**12**(10):617.

https://doi.org/10.3390/toxins12100617.

Holford M, Daly M, King GF, Norton RS. Venoms to the rescue. *Science*. 2018:**361**(6405):842–844. https://doi.org/10.1126/science.aau7761.

Houle D, Rossoni DM. Complexity, evolvability, and the process of adaptation. *Annual Review of Ecology, Evolution, and Systematics*. 2022: **53**:137–159. https://doi.org/10.1146/annurev-ecolsys-102320-090809.

Jansa SA, Voss RS. Adaptive evolution of the venom-targeted vWF protein in opossums that eat pitvipers. *PLOS One*. 2011:**6**(6):e20997. https://doi.org/10.1371/journal.pone.0020997.

Jones P, Binns D, Chang HY, Fraser M, Li W, McAnulla C, McWilliam H, Maslen J, Mitchell A, Nuka G, *et al.* InterProScan 5: genome-scale protein function classification. *Bioinformatics*. 2014:**30**(9):1236–1240. https://doi.org/10.1093/bioinformatics/btu031.

Kessner D, Novembre J. Power analysis of artificial selection experiments using efficient whole genome simulation of quantitative traits. *Genetics*. 2015:**199**(4):991–1005. https://doi.org/10.1534/genetics.115.175075.

Khalil S, Jacobson E, Chambers MC, Lazzaro BP. Systemic bacterial infection and immune defense phenotypes in *Drosophila melanogaster*. *JoVE (Journal of Visualized Experiments)*. 2015: **99**:e52613. https://doi.org/10.3791/52613.

Kikkawa T, Osumi N. Multiple functions of the *Dmrt* genes in the development of the central nervous system. *Frontiers in Neuroscience*. 2021:**15**:789583. https://doi.org/10.3389/fnins.2021.789583.

Kim D, Langmead B, Salzberg SL. HISAT: a fast spliced aligner with low memory requirements. *Nature Methods*. 2015:**12**(4):357–360. https://doi.org/10.1038/nmeth.3317.

King EG, Macdonald SJ, Long AD. Properties and power of the *Drosophila* Synthetic Population Resource for the routine dissection of complex traits. *Genetics*. 2012a:**191**(3):935–949. https://doi.org/10.1534/genetics.112.138537.

King EG, Merkes CM, McNeil CL, Hoofer SR, Sen S, Broman KW, Long AD, Macdonald SJ. Genetic dissection of a model complex trait using the *Drosophila* Synthetic Population Resource. *Genome Research*. 2012b:**22**(8):1558–1566. https://doi.org/10.1101/gr.134031.111.

Knapp O, Stiles B, Popoff MR. The aerolysin-like toxin family of cytolytic, pore-forming toxins. *The Open Toxinology Journal*. 2010:**3**(1):53–68. https://dx.doi.org/10.2174/1875414701003010053.

Kofler R, Pandey RV, Schlötterer C. PoPoolation2: identifying differentiation between populations using sequencing of pooled DNA samples (Pool-Seq). *Bioinformatics*. 2011:**27**(24):3435–3436. https://doi.org/10.1093/bioinformatics/btr589.

Kofler R, Schlötterer C. Gowinda: unbiased analysis of gene set enrichment for genome-wide association studies. *Bioinformatics*. 2012:**28**(15):2084–2085. https://doi.org/10.1093/bioinformatics/bts315.

Kofler R, Schlötterer C. A guide for the design of evolve and resequencing studies. *Molecular Biology and Evolution*. 2014:**31**(2):474–483. https://doi.org/10.1093/molbev/mst221.

Kurlovs AH, Snoeck S, Kosterlitz O, Van Leeuwen T, Clark RM. Trait mapping in diverse arthropods by bulked segregant analysis. *Current Opinion in Insect Science*. 2019:**36**:57–65. https://doi.org/10.1016/j.cois.2019.08.004.

Laetsch DR, Blaxter ML. BlobTools: interrogation of genome assemblies. *F1000Research*. 2017:**6**:1287. https://doi.org/10.12688/f1000research.12232.1.

Lau MT, Manion J, Littleboy JB, Oyston L, Khuong TM, Wang QP, Nguyen DT, Hesselson D, Seymour JE, Neely GG. Molecular dissection of box jellyfish venom cytotoxicity highlights an effective venom antidote. *Nature Communications*. 2019:**10**:1655. https://doi.org/10.1038/s41467-019-09681-1.

Lenski RE. Coevolution of bacteria and phage: are there endless cycles of bacterial defenses and phage counterdefenses? *Journal of Theoretical Biology*. 1984:**108**(3):319–325. https://doi.org/10.1016/S0022-5193(84)80035-1.

Li H. A statistical framework for SNP calling, mutation discovery, association mapping and population genetical parameter estimation from sequencing data. *Bioinformatics*. 2011:**27**(21):2987–2993. https://doi.org/10.1093/bioinformatics/btr509.

Li H. Aligning sequence reads, clone sequences and assembly contigs with BWA-MEM. *arXiv preprint arXiv:13033997*. 2013: https://doi.org/10.48550/arXiv.1303.3997.

Li H, Durbin R. Fast and accurate short read alignment with Burrows-Wheeler transform. *Bioinformatics*. 2009:**25**(14):1754–1760. https://doi.org/10.1093/bioinformatics/btp324.

Li H, Handsaker B, Wysoker A, Fennell T, Ruan J, Homer N, Marth G, Abecasis G, Durbin R. The sequence alignment/map format and SAMtools. *Bioinformatics*. 2009:**25**(16):2078–2079. https://doi.org/10.1093/bioinformatics/btp352.

Luo A, Wang A, Kamau PM, Lai R, Luo L. Centipede venom: a potential source of ion channel modulators. *International Journal of Molecular Sciences*. 2022:**23**(13):7105. https://doi.org/10.3390/ijms23137105.

Luo L, Li B, Wang S, Wu F, Wang X, Liang P, Ombati R, Chen J, Lu X, Cui J, *et al.* Centipedes subdue giant prey by blocking KCNQ channels. *Proceedings of the National Academy of Sciences*. 2018:**115**(7):1646–1651. https://doi.org/10.1073/pnas.1714760115.

Mank JE. Population genetics of sexual conflict in the genomic era. *Nature Reviews Genetics*. 2017:**18**(12):721–730. https://doi.org/10.1038/nrg.2017.83.

Margres MJ, McGivern JJ, Seavy M, Wray KP, Facente J, Rokyta DR. Contrasting modes and tempos of venom expression evolution in two snake species. *Genetics*. 2015:**199**:165–176. https://doi.org/10.1534/genetics.114.172437.

Margres MJ, Patton A, Wray KP, Hassinger ATB, Ward MJ, Lemmon EM, Lemmon AR, Rokyta DR. Tipping the scales: the migration-selection balance leans toward selection in snake venoms. *Molecular Biology and Evolution*. 2019:**36**(2):271–282. https://doi.org/10.1093/molbev/msy207.

Margres MJ, Rautsaw RM, Strickland JL, Mason AJ, Schramer TD, Hofmann EP, Stiers E, Ellsworth SA, Nystrom GS, Hogan MP, *et al.* The tiger rattlesnake genome reveals a complex genotype underlying a simple venom phenotype. *Proceedings of the National Academy of Sciences*. 2021:**118**(4):e2014634118. https://doi.org/10.1073/pnas.2014634118.

Margres MJ, Wray KP, Hassinger AT, Ward MJ, McGivern JJ, Moriarty Lemmon E, Lemmon AR, Rokyta DR. Quantity, not quality: rapid adaptation in a polygenic trait proceeded exclusively through expression differentiation. *Molecular Biology and Evolution*. 2017:**34**(12):3099–3110. https://doi.org/10.1093/molbev/msx231.

Märkle H, John S, Cornille A, Fields PD, Tellier A. Novel genomic approaches to study antagonistic coevolution between hosts and parasites. *Molecular Ecology*. 2021:**30**:3660–3676. https://doi.org/10.1111/mec.16001.

Marriage TN, King EG, Long AD, Macdonald SJ. Fine-mapping nicotine resistance loci in *Drosophila* using a multiparent advanced generation inter-cross population. *Genetics*. 2014:**198**(1):45–57. https://doi.org/10.1534/genetics.114.162107.

Martin M. Cutadapt removes adapter sequences from high-throughput sequencing reads. *EMBnetjournal*. 2011:**17**(1):10–12. https://doi.org/10.14806/ej.17.1.200.

McGee LW, Sackman AM, Morrison AJ, Pierce J, Anisman J, Rokyta DR. Synergistic pleiotropy overrides the costs of complexity in viral adaptation. *Genetics*. 2016:**202**:285–295. https://doi.org/10.1534/genetics.115.181628.

McGlothlin JW, Kobiela ME, Feldman CR, Castoe TA, Geffeney SL, Hanifin CT, Toledo G, JVonk F, Richardson MK, Brodie Jr ED, *et al.* Historical contingency in a multigene family facilitates adaptive evolution of toxin resistance. *Current Biology*. 2016:**26**(12):1616–1621. https://doi.org/10.1016/j.cub.2016.04.056.

McKenna A, Hanna M, Banks E, Sivachenko A, Cibulskis K, Kernytsky A, Garimella K, Altshuler D, Gabriel S, Daly M, *et al.* The Genome Analysis Toolkit: a MapReduce framework for analyzing next-generation DNA sequencing data. *Genome Research*. 2010:**20**(9):1297–1303. https://doi.org/10.1101/gr.107524.110.

Medina M, Baker DM, Baltrus DA, Bennett GM, Cardini U, Correa AMS, Degnan SM, Christa G, Kim E, Li J, *et al.* Grand challenges in coevolution. *Frontiers in Ecology and Evolution*. 2022:**9**:618251. https://doi.org/10.3389/fevo.2021.618251.

Monge-Fuentes V, Arenas C, Galante P, Gonçalves JC, Mortari MR, Schwartz EF. Arthropod toxins and their antinociceptive properties: from venoms to painkillers. *Pharmacology and Therapeutics*. 2018:**188**:176–185. https://doi.org/10.1016/j.pharmthera.2018.03.007.

Morrow EH, Connallon T. Implications of sex-specific selection for the genetic basis of disease. *Evolutionary Applications*. 2013:**6**(8):1208–1217. https://doi.org/10.1111/eva.12097.

Myers EA, Strickland JL, Rautsaw RM, Mason AJ, Schramer TD, Nystrom GS, Hogan MP, Yooseph S, Rokyta DR, Parkinson CL. *De novo* genome assembly highlights the role of lineage-specific gene duplications in the evolution of venom in Fea's viper (*Azemiops feae*). *Genome Biology and Evolution*. 2022:**17**:evaf033. https://doi.org/10.1093/gbe/evaf033.

Nachtigall PG, Nystrom GS, Broussard EM, Wray KP, de Azevedo ILMJ, Parkinson CL, Margres MJ, Rokyta DR. A segregating structural variant defines novel venom phenotypes in the eastern diamondback rattlesnake. *Molecular Biology and Evolution*. 2025:**42**:msaf058. https://doi.org/10.1093/molbev/msaf058.

Ng'oma E, Fidelis W, Middleton KM, King EG. The evolutionary potential of diet-dependent effects on lifespan and fecundity in a multi-parental population of *Drosophila melanogaster*. *Heredity*. 2019:**122**(5):582. https://doi.org/10.1038/s41437-018-0154-2.

Nuzhdin SV, Turner TL. Promises and limitations of hitchhiking mapping. *Current Opinion in Genetics and Development*. 2013:**23**(6):694–699. https://doi.org/10.1016/j.gde.2013.10.002.

Nystrom GS, Ward MJ, Ellsworth SA, Rokyta DR. Sex-based venom variation in the eastern bark centipede (*Hemiscolopendra marginata*). *Toxicon*. 2019:**169**:45–58. https://doi.org/10.1016/j.toxicon.2019.08.001.

Orozco-Terwengel P, Kapun M, Nolte V, Kofler R, Flatt T, Schlötterer C. Adaptation of *Drosophila* to a novel laboratory environment reveals temporally heterogeneous trajectories of selected alleles. *Molecular Ecology*. 2012:

21(20):4931–4941. https://doi.org/10.1111/j.1365-294X.2012.05673.x.

Orr HA. Adaptation and the cost of complexity. *Evolution*. 2000:**54**:13–20. https://doi.org/10.1111/j.0014-3820.2000.tb00002.x.

Parchman TL, Benkman CW. Diversifying coevolution between crossbills and black spruce on Newfoundland. *Evolution*. 2002:**56**(8):1663–1672. https://doi.org/10.1111/j.0014-3820.2002.tb01478.x.

Pertea G, Pertea M. GFF utilities: GffRead and GffCompare. *F1000Research*. 2020:**9**. https://doi.org/10.12688/f1000research.23297.2.

Pertea M, Kim D, Pertea GM, Leek JT, Salzberg SL. Transcript-level expression analysis of RNA-seq experiments with HISAT, StringTie and Ballgown. *Nature Protocols*. 2016:**11**(9):1650–1667. https://doi.org/10.1038/nprot.2016.095.

Pertea M, Pertea GM, Antonescu CM, Chang TC, Mendell JT, Salzberg SL. StringTie enables improved reconstruction of a transcriptome from RNA-seq reads. *Nature Biotechnology*. 2015:**33**(3):290–295. https://doi.org/10.1038/nbt.3122.

Pertoldi C, A Bach L, SF Barker J, Lundberg P, Loeschcke V. The consequences of the variance-mean rescaling effect on effective population size. *Oikos*. 2007:**116**(5):769–774. https://doi.org/10.1111/j.0030-1299.2007.15672.x.

Poplin R, Ruano-Rubio V, DePristo MA, Fennell TJ, Carneiro MO, Van der Auwera GA, Kling DE, Gauthier LD, Levy-Moonshine A, Roazen D, *et al.* Scaling accurate genetic variant discovery to tens of thousands of samples. *BioRxiv*. 2017:**N/A**:201178. https://doi.org/10.1101/201178.

Robinson SD, Deuis JR, Klasfauseweh T, Schendel V, Vetter I. Venom-derived pain-causing toxins: insights into sensory neuron function and pain mechanisms. *Pain*. 2022:**163**(S1):S46–S56. 10.1097/j.pain.0000000000002701.

Rokyta DR, Lemmon AR, Margres MJ, Aronow K. The venom-gland transcriptome of the eastern diamondback rattlesnake (*Crotalus adamanteus*). *BMC Genomics*. 2012:**13**:312. https://doi.org/10.1186/1471-2164-13-312.

Rostant WG, Kay C, Wedell N, Hosken DJ. Sexual conflict maintains variation at an insecticide resistance locus. *BMC Biology*. 2015:**13**(1):34. https://doi.org/10.1186/s12915-015-0143-3.

Rowe AH, Xiao Y, Rowe MP, Cummins TR, Zakon HH. Voltage-gated sodium channel in grasshopper mice defends against bark scorpion toxin. *Science*. 2013:**342**(6157):441–446. https://doi.org/10.1126/science.1236451.

Royston JP. An extension of Shapiro and Wilk's W test for normality to large samples. *Journal of the Royal Statistical Society: Series C (Applied Statistics)*. 1982:**31**(2):115–124. https://doi.org/10.2307/2347973.

Sackman AM, Rokyta DR. No cost of complexity in bacteriophages adapting to a complex environment. *Genetics*. 2019:**212**:267–276. https://doi.org/10.1534/genetics.119.302029.

Schenker N, Gentleman JF. On judging the significance of differences by examining the overlap between confidence intervals. *The American Statistician*. 2001:**55**(3):182–186. https://doi.org/10.1198/000313001317097960.

Schlötterer C, Kofler R, Versace E, Tobler R, Franssen S. Combining experimental evolution with next-generation sequencing: a powerful tool to study adaptation from standing genetic variation. *Heredity*. 2015:**114**(5):431–440. https://doi.org/10.1038/hdy.2014.86.

Simão FA, Waterhouse RM, Ioannidis P, Kriventseva EV, Zdobnov EM. BUSCO: assessing genome assembly and annotation completeness with single-copy orthologs. *Bioinformatics*. 2015:**31**(19):3210–3212. https://doi.org/10.1093/bioinformatics/btv351.

Smit A, Hubley R. Repeatmodeler open-1.0 http://www. repeatmasker. org. 2008.

Smit A, Hubley R, Green P. Repeat-masker open-4.0. *http://wwwrepeatmaskerorg*. 2013–2015:.

Smith JW, Benkman CW. A coevolutionary arms race causes ecological speciation in crossbills. *American Naturalist*. 2007:**169**(4):455–465. https://doi.org/10.1086/511961.

Stone, Brenton R. *tsk: Trimmed Spearman-Karber Method*. 2015.

Taus T, Futschik A, Schlötterer C. Quantifying selection with Pool-Seq time series data. *Molecular Biology and Evolution*. 2017:**34**(11):3023–3034. https://doi.org/10.1093/molbev/msx225.

Terhorst J, Schlötterer C, Song YS. Multi-locus analysis of genomic time series data from experimental evolution. *PLoS Genetics*. 2015:**11**(4). https://doi.org/10.1371/journal.pgen.1005069.

Thompson JN. *The Geographic Mosaic of Coevolution*. University of Chicago Press, Chicago. 2005.

Thompson JN. *Relentless Evolution*. University of Chicago Press. 2013.

Thurmond J, Goodman JL, Strelets VB, Attrill H, Gramates LS, Marygold SJ, Matthews BB, Millburn G, Antonazzo G, Trovisco V, *et al.* Flybase 2.0: the next generation. *Nucleic Acids Research*. 2019:**47**(D1):D759–D765. https://doi.org/10.1093/nar/gky1003.

Toju H. Fine-scale local adaptation of weevil mouthpart length and camellia pericarp thickness: Altitudinal gradient of a putative arms race. *Evolution*. 2008:**62**(5):1086–1102. https://doi.org/10.1111/j.1558-5646.2008.00341.x.

Van der Auwera GA, Carneiro MO, Hartl C, Poplin R, Del Angel G, Levy-Moonshine A, Jordan T, Shakir K, Roazen D, Thibault J, *et al.* From FastQ data to high-confidence variant calls: the Genome Analysis Toolkit best practices pipeline. *Current Protocols in Bioinformatics*. 2013:**43**(1):11–10. https://doi.org/10.1002/0471250953.bi1110s43.

Vlachos C, Burny C, Pelizzola M, Borges R, Futschik A, Kofler R, Schlötterer C. Benchmarking software tools for detecting and quantifying selection in evolve and resequencing studies. *Genome Biology*. 2019:**20**(1):169. https://doi.org/10.1186/s13059-019-1770-8.

Vlachos C, Kofler R. MimicrEE2: genome-wide forward simulations of evolve and resequencing studies. *PLoS Computational Biology*. 2018:**14**(8):e1006413. https://doi.org/10.1371/journal.pcbi.1006413.

Wagner GP, Kenney-Hunt JP, Pavlicev M, Peck JR, Waxman D, Cheverud JM. Pleiotropic scaling of gene effects and the 'cost of complexity'. *Nature*. 2008:**452**:470–473. https://doi.org/10.1038/nature06756.

Wang Z, Liao BY, Zhang J. Genomic patterns of pleiotropy and the evolution of complexity. *Proceedings of the National Academy of Sciences*. 2010:**107**:18034–18039. https://doi.org/10.1073/pnas.1004666107.

Ward MJ, Ellsworth SA, Hogan MP, Nystrom GS, Martinez P, Budhdeo A, Zelaya R, Perez A, Powell B, He H, *et al.* Female-biased population divergence in the venom of the Hentz striped scorpion (*Centruroides hentzi*). *Toxicon*. 2018a:**152**:137–149. https://doi.org/10.1016/j.toxicon.2018.07.026.

Ward MJ, Ellsworth SA, Rokyta DR. Venom-gland transcriptomics and venom proteomics of the Hentz striped scorpion (*Centruroides hentzi*; Buthidae) reveal high toxin diversity in a harmless member of a lethal family. *Toxicon*. 2018b:**142**:14–29. https://doi.org/10.1016/j.toxicon.2017.12.042.

Ward MJ, Rokyta DR. Venom-gland transcriptomics and venom proteomics of the giant Florida blue centipede, *Scolopendra viridis*. *Toxicon*. 2018:**152**:121–136. https://doi.org/10.1016/j.toxicon.2018.07.030.

Wellenreuther M, Hansson B. Detecting polygenic evolution: Problems, pitfalls, and promises. *Trends in Genetics*. 2016:**32**(3):155–164. https://doi.org/10.1016/j.tig.2015.12.004.

Wheeler KP, Watt DD, Lazdunski M. Classification of Na channel receptors specific for various scorpion toxins. *Pflügers Archiv European Journal of Physiology*. 1983:**397**(2):164–165. https://doi.org/10.1007/bf00582058.

Ye X, Yan Z, Yang Y, Xiao S, Chen L, Wang J, Wang F, Xiong S, Mei Y, Wang F, *et al.* A chromosome-level genome assembly of the parasitoid wasp *Pteromalus puparum*. *Molecular Ecology Resources*. 2020:**20**(5):1384–1402. https://doi.org/10.1111/1755-0998.13206.

Zhou S, Luoma SE, St Armour GE, Thakkar E, Mackay TF, Anholt RR. A *Drosophila* model for toxicogenomics: genetic variation in susceptibility to heavy metal exposure. *PLoS Genetics*. 2017:**13**(7):e1006907. https://doi.org/10.1371/journal.pgen.1006907.

Zuk M, McKean KA. Sex differences in parasite infections: Patterns and processes. *International Journal for Parasitology*. 1996:**26**:1009–1024. https://doi.org/10.1016/S0020-7519(96)80001-4.